

Long-Term Photometry of IC 348 with the YETI Network

D. J. Fritzewski,^{1,2*} M. Kitze,¹ M. Mugrauer,¹ R. Neuhäuser,¹
 C. Adam,¹ C. Briceño,³ S. Buder,^{1,4} T. Butterley,⁵ W.-P. Chen,⁶ B. Dincel,^{1,7}
 V. S. Dhillon,^{8,9} R. Errmann,^{1,10} Z. Garai,¹¹ H. F. W. Gilbert,¹ C. Ginski,^{1,12}
 J. Greif,¹ L. K. Hardy,⁸ J. Hernández,^{13,14} P. C. Huang,⁶ A. Kellerer,¹⁵ E. Kundra,¹¹
 S. P. Littlefair,⁸ M. Mallonn,² C. Marka,^{1,16} A. Pannicke,¹ T. Pribulla,¹¹ St. Raetz,^{1,17}
 J. G. Schmidt,^{1,18} T. O. B. Schmidt,^{1,19} M. Seeliger,¹ R. W. Wilson,⁵ and V. Wolf¹

¹*Astrophysikalisches Institut und Universitäts-Sternwarte Friedrich-Schiller-Universität Jena, Schillergässchen 2-3, 07745 Jena, Germany*

²*Leibniz-Institut für Astrophysik (AIP), An der Sternwarte 16, 14482 Potsdam, Germany*

³*Cerro Tololo Interamerican Observatory, Casilla Postal 603, La Serena 1700000, Chile*

⁴*Max-Planck-Institut für Astronomie, Königstuhl 17, 69117 Heidelberg, Germany*

⁵*Centre for Advanced Instrumentation, Department of Physics, University of Durham, South Road, Durham DH1 3LE, UK*

⁶*Graduate Institute of Astronomy, National Central University, 300 Jhongda Road, Jhongli 32001, Taiwan*

⁷*Institut für Astronomie und Astrophysik Tübingen, Sand 1, 72076 Tübingen, Germany*

⁸*Department of Physics and Astronomy, University of Sheffield, Sheffield S3 7RH, UK*

⁹*Instituto de Astrofísica de Canarias, 38205 La Laguna, Tenerife, Spain*

¹⁰*Abbe School of Photonics, Max-Wien-Platz 1, 07743 Jena, Germany*

¹¹*Astronomical Institute, Slovak Academy of Sciences, 059 60 Tatranská Lomnica, Slovakia*

¹²*Leiden Observatory, Leiden University, PO Box 9513, 2300 RA Leiden, the Netherlands*

¹³*Centro de Investigaciones de Astronomía, Apdo. Postal 264, Mérida 5101-A, Venezuela*

¹⁴*Instituto de Astronomía, Universidad Nacional Autónoma de México, Unidad Académica en Ensenada, Ensenada 22860, México*

¹⁵*Battcock Centre for Experimental Astrophysics, Cavendish Laboratory, Cambridge University, JJ Thompson Avenue, Cambridge, CB3 0HE, UK*

¹⁶*Instituto Radioastronomía Milimétrica (IRAM), Avenida Divina Pastora 7, E-18012 Granada, Spain*

¹⁷*ESTEC - SCI-S ESA - European Space Agency, Keplerlaan 1, 2201 AZ Noordwijk, The Netherlands*

¹⁸*Theoretische Astrophysik, Universität Tübingen, Auf der Morgenstelle 10, 72076 Tübingen, Germany*

¹⁹*Hamburger Sternwarte, Gojenbergsweg 112, 21029 Hamburg, Germany*

Accepted XXX. Received YYY; in original form ZZZ

ABSTRACT

We present long-term photometric observations of the young open cluster IC 348 with a baseline time-scale of 2.4 yr. Our study was conducted with several telescopes from the Young Exoplanet Transit Initiative (YETI) network in the Bessel *R* band to find periodic variability of young stars. We identified 87 stars in IC 348 to be periodically variable; 33 of them were unreported before. Additionally, we detected 61 periodic non-members of which 41 are new discoveries. Our wide field of view was the key to those numerous newly found variable stars. The distribution of rotation periods in IC 348 has always been of special interest. We investigate it further with our newly detected periods but we cannot find a statistically significant bimodality. We also report the detection of a close eclipsing binary in IC 348 composed of a low-mass stellar component ($M \gtrsim 0.09 M_{\odot}$) and a K0 pre-main sequence star ($M \approx 2.7 M_{\odot}$). Furthermore, we discovered three detached binaries among the background stars in our field of view and confirmed the period of a fourth one.

Key words: stars: variables: general – stars: variables: T Tauri – starspots – binaries: eclipsing – open clusters and associations: individual: IC 348 – techniques: photometric

1 INTRODUCTION

The transit technique for finding planetary candidates is applied in several ground-based (e.g. Bakos et al. 2004 and

* E-mail: dfritzewski@aip.de

Nutzman & Charbonneau 2008) and space-based surveys (e.g. Bordé et al. 2003 and Ricker et al. 2014). This work is part of a project within the ground-based Young Exoplanet Transit Initiative (YETI) (Neuhäuser et al. 2011). We used the data obtained by this survey to search for general periodic variation in the young open cluster IC 348. For an overview on the current state of YETI we refer the reader to the recent work of Garai et al. (2016).

In this paper we focus on the young (2 Myr, Luhman et al. 2003), nearby (316 pc, Herbig 1998), and compact ($D \sim 20'$, Luhman et al. 2003) open cluster IC 348. It is an intensely studied region of ongoing star formation. The T-Tauri stars (TTS) found therein by Herbig (1954) played an important role in the exploration of star formation (Herbig 1998). The theory that TTS are young was strengthened and later confirmed through colour measurements and theoretical evolutionary models with the help of those TTS.

It is well known that IC 348 is younger than 10 Myr but its age and the age-spread are still under debate. Luhman et al. (1998) found an age spread from 0.5 Myr to 10 Myr from the photometric scatter in the colour-magnitude diagram. A similar wide age-spread was assumed in the Orion Nebula Cluster but it was shown by Jeffries et al. (2011) that observational and physical effects give rise to the observed luminosity dispersion. Because of the observed colour spread in IC 348 Bell et al. (2013) argues for an age of 6 Myr for IC 348 while (Luhman et al. 2003) adopted a median age of 2 Myr which we use in this work.

The stellar content of IC 348 was researched with the photometric studies by Herbig (1998) and Luhman et al. (1998). With the help of the proper motion measurements from Scholz et al. (1999) and additional photometric and spectroscopic data Luhman et al. (2003) compiled a membership catalogue of IC 348, including spectral classification for most of its members. This catalogue has recently been extended by Luhman et al. (2016) to include 478 members. The membership criterion was based on proper motion, position on the colour-magnitude diagram, and spectral features and classification.

Using CCD detectors, photometric time-series of different durations and with different fields of view (FoV), but all in the I band, have been obtained and published. The first time-series of its kind of IC 348 was published by Herbst et al. (2000b) with a baseline time-scale of four months. The FoV was $10.2' \times 10.2'$ and the authors found 19 periodic variable stars near the centre of the cluster. With more data from the same survey, Cohen et al. (2004) were able to detect 28 periodic variables. Finally, with a baseline of seven years, Nordhagen et al. (2006a) found twelve additional periodic stars in the same FoV. An independent study with deeper photometry was published by Littlefair et al. (2005) and found 32 new periodic variables in IC 348. The most extensive study so far has been conducted by Cieza & Baliber (2006). The authors used a wider FoV ($46.2' \times 46.2'$) and were able to discover 75 additional periodic variables. Moreover, they combined and analysed all previous studies and counted a total of 106 periodic stars among the members of IC 348 when applying the membership of Luhman et al. (2016).

The evolution of angular momentum in young stars is a topic of recent research (e.g. Tanveer Karim et al. 2016) and the distribution of rotation periods is a stepping stone to its

understanding. Since the discovery of a bimodal period distribution for stars with $M > 0.25M_{\odot}$ in the 1 Myr old Orion Nebula Cluster (ONC) by Attridge & Herbst (1992) other open clusters are compared to this young cluster. IC 348 is slightly older and the previous time-series studies came to the conclusion that the period distributions of both clusters look alike. The distribution consists of fast rotators with periods of ~ 2 d and slow rotators with periods of ~ 8 d. With more rotational periods for the members of IC 348 we can investigate the distribution in more detail.

In this study, carried out within the YETI network we used an even wider FoV ($52.8' \times 52.8'$) than any previous studies. With this FoV we can find variabilities in IC 348 and its vicinity. Moreover, we used several telescopes located all over the world to achieve a better phase coverage of our time-series.

The paper starts with an overview of our observations and the data reduction workflow (section 2). Thereafter, we present the results (section 3), starting with variables in IC 348, followed by further results on field stars. In the discussion (section 4) we compare our results with previous studies.

2 OBSERVATIONS AND DATA REDUCTION

2.1 Observations

IC 348 was observed between 2012 August 22 and 2015 January 18 in 125 telescopic nights over three seasons. Observations were carried out by nine telescopes through the YETI network, with a distributed longitudinal coverage (Table 1). The University Observatory Jena alone contributed 88 nights. Details on all observations can be found in Table 2. To achieve a good phase coverage three week-long YETI campaigns were performed in which IC 348 was observed from the participating observatories on every clear night. Therefore continuous coverage of IC 348 could be achieved at some nights through combined observations. Overall, the distributed observations resulted in a better phase-coverage of the data. In Figure 1 we compare the phase-coverage of YETI data to Jena data alone and the advantage of YETI is clearly visible. For easier interpretation of Figure 1 we show the deviation of the curves in addition to the data. The combined light curves, compiled from all telescopes, have better phase-coverage in the range of 10 d to 25 d (25 percentage points) and for periods of the multiple of one day (up to 35 percentage points). The better phase-coverage for multiple periods of one day reduces the 1 d alias period significantly when searching for periods.

In Jena the open cluster was observed with the 0.6 m Schmidt telescope. We used the Schmidt-Teleskop-Kamera (STK) (Mugrauer & Berthold 2010) with its Bessel R filter and exposed for 50 s. The exposure times at other telescopes differed because of different apertures, smaller FoV, and other detectors. Additional BVI images were acquired on some nights at the University Observatory Jena. Further observations were carried out with the 0.25 m Cassegrain telescope equipped with the Cassegrain-Teleskop-Kamera II (CTK-II) (Mugrauer 2016) at the University Observatory Jena. For those observations we used Bessel V and I filters and exposed for 180 s.

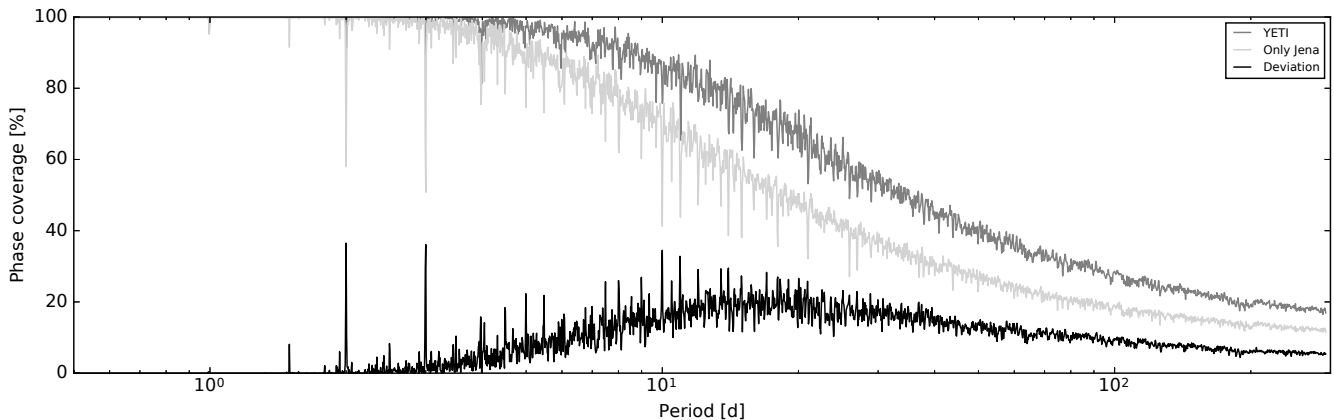


Figure 1. Phase coverage of the data for a single star. The dark grey line includes all YETI observations while the light grey line gives the phase coverage for the observations from the University Observatory Jena. In black the difference of both curves is shown for easier interpretation. The better phase-coverage for periods of the multiple of one day is clearly visible (spikes), as well as the big advantage for periods in the range of 10 d to 25 d.

Table 1. Overview of the YETI telescopes used for this work. FoV stands for field of view. In Stará Lesná two 0.6 m telescopes have been used with different detectors. The table is sorted by the number of obtained frames.

Observatory	Telescope	Longitude [°]	Latitude [°]	FoV [']	# Frames	CCD Detector	Pixel scale ["/ px]
Jena ^a	0.6 m Schmidt	11.48416 E	50.92888 N	52.8 × 52.8	10 808	e2v 42-10	1.547
Jena ^b	0.25 Cassegrain	11.48416 E	50.92888 N	21.0 × 20.4	2390	e2v 47-10	1.193
Stará Lesná	0.6 m Cassegrain	20.29081 E	49.15207 N	14 × 14	1957	FLI ML3048	0.410
				16.9 × 16.9		MI G4-9000	0.333
pt5m, La Palma ^c	0.5 m mod. Dall-Kirkham	17.88188 W	28.76058 N	10.2 × 6.9	1 050	KAF-3200ME	0.280
Lulin	1 m Cassegrain	120.87297 E	23.46908 N	11.5 × 11.2	614	e2v 36-40	0.515
Tenagra	0.8 m Ritchey-Chrétien	110.98475 W	31.55571 N	14.8 × 14.8	584		0.867
Saitama	0.55 m Ritchey-Chrétien	139.60561 E	35.86225 N	12.8 × 12.4	218	ML4710-1	0.727
Swarthmore	0.6 m Ritchey-Chrétien	75.35605 W	39.90702 N	26 × 26	195	Apogee U16M	0.381
Llano del Hato	1 m Cassegrain-Coudé	70.87094 W	8.78794 N	18.5 × 18.5	30	e2v 42-40	0.542

References: ^aMugrauer & Berthold (2010), ^bMugrauer (2016), ^cHardy et al. (2015)

Table 2. Observational seasons and number of nights with successful observations.

Season	Date	Number of nights
1	2012 Aug. 8 – 2013 Mar. 15	57
2	2013 Aug. 1 – 2014 Feb. 4	41
3	2014 Sep. 16 – 2015 Jan. 18	27

In addition to the Jena telescopes we observed with the pt5m telescope on La Palma (Hardy et al. 2015), the 1 m Cassegrain at the LOT observatory in Lulin, the 1 m Cassegrain-Coudé in Llano del Hato, the two 0.6 m Cassegrain in Stará Lesná, and the Ritchey-Chrétien telescopes of Saitama University, Swarthmore College, and Tenagra observatory. The locations, diameters, and detectors of all telescopes used can be found in Table 1.

Most data were gathered with the STK operated at the Jena 0.6 m Schmidt telescope, therefore the stars which were analysed are all in the FoV of this telescope. Additionally, the STK exhibits the widest FoV of all instruments used. Some telescopes obtained images with deeper photometry.

We decided not to use the additional fainter stars from those frames. The sparse coverage of the light curve would not have given insight to the time-scale we are interested in.

The STK is equipped with a 2048 px × 2048 px e2v CCD detector with a FoV of 52.8' × 52.8' (Mugrauer & Berthold 2010). The centre of IC 348 was positioned slightly off the centre of the detector to north-east to allow simultaneous observations with the CTK-II (centred at $\alpha = 3^{\text{h}} 45^{\text{m}} 20^{\text{s}}$, $\delta = +32^{\circ} 4' 50''$). From this FoV the 1001 brightest stars have been analysed independent of their membership status down to a limiting magnitude of $R = (18.7 \pm 0.3)$ mag. Within our sample 137 stars are members of IC 348 according to Luhman et al. (2016). Further stars are either unidentified members, background or foreground stars.

All other telescopes used for this observations have a smaller FoV. Therefore, they included a tighter area around IC 348 or covered the whole region with various pointings, which implies that not all stars of our selection have been observed by all telescopes.

The FoV of the STK is shown in Figure 2 as a composite image of B , V , and R observations. It is dominated by the bright star Atik (o Per). The open cluster IC 348 lies south

of it and is surrounded by a reflection nebula. In this frame we marked our observed stars according to their properties.

2.2 Data reduction and photometry

For every night, in addition to the science frames, darks and flats were obtained. Whenever possible we acquired sky flats, otherwise the nightly dome flats were used. Some telescopes included the bias in an overscan region while others produced dedicated bias frames. From those images a standard reduction with dark, bias, and flat field correction was performed with IRAF.

For every telescopic pointing the data were extracted separately from the reduced images with aperture photometry followed by differential photometry. For the differential photometry we used an implementation of the algorithm presented by Broeg et al. (2005), based on the IRAF task PHOT as described in detail in Errmann et al. (2014). This algorithm calculates an artificial star for comparison from all stars in the FoV, weighted according to the standard deviation of the differential light curves. From this procedure we obtained a light curve for each pointing on each night.

In Figure 3 the mean photometric precision of one night is shown. The winter night of 2014 December 8 is exemplary and represents the normal conditions achieved at the University Observatory Jena. E.g. for a 16 mag star a photometric precision of 0.03 mag is reached.

After combining the data for each telescope, by adjusting the flux level from night to night, we had to collate all observations of each star obtained with different telescopes. For this step we first searched for periodic variations in the light curves from the Jena observations using the algorithms presented in subsection 2.3. Thereafter, we used the periods to produce phase-folded light curves. Because of the tighter sampling in the phase domain the data from other telescopes can easily be incorporated into the light curve. This was done by adjusting the flux of the observations to the flux of the data with similar phases. The very good phase-coverage of the Jena data was mandatory for this method.

With only a few nights of multi-band photometry we decided to anchor our photometry to Trullols & Jordi (1997). We used the night of 2014 December 8 for the transformation and all magnitudes used in the current work are based on this system.

2.3 Algorithms used to find periodic variabilities

The main goal of this work was to find new periodic photometric variables in IC 348 and to confirm and improve ephemerides of already known variable stars in this cluster. Therefore we applied three different algorithms to detect periodicities in the data. All algorithms have in common that they use a grid of fixed periods as their input. We employed the same grid for all algorithms to gain comparable results.

This period grid had a range from $P_{\min} = 0.04$ d (~ 1 h) to $P_{\max} = T/3 = 293$ d (where T is our observational timebase). We used such a wide range because at least one long-periodic eclipse is known in IC 348 (Nordhagen et al. 2006b) and more might be discovered. We chose our lower limit to include short-term variability but not stellar pulsations. The upper limit was guided by the decision to include at least three

cycles. To save computation time we used an exponentially-spaced grid with $n \sim 38000$ points. The resolution of the grid is for the lower limit 1 s, for a period of 1 d 20 s and for the upper limit of 293 d 1.6 h.

The first algorithm we used is the widely applied generalized Lomb-Scargle (GLS) periodogram by Zechmeister & Kürster (2009). From the periodogram we obtained the spectral power density as a measurement of the certainty of the periodic variations. Although the algorithm is fast and convenient for finding periods it has some drawbacks. It favours signals with sinusoidal shape which can lead to incorrect best-fitting values for non-sinusoidal-shaped light curves like transits, occultations or eclipsing binaries.

As a second algorithm the minimal string-length algorithm by Dworetsky (1983) was used. Unlike the GLS a string-length algorithm can find periodic variabilities of all shapes with the same sensitivity. In this algorithm the sum of the distances of succeeding points in the phase-folded representation is measured. Because of lower phase-coverage for long periods this method is biased towards longer periods. To correct this effect a sum of a second-order polynomial and an exponential decay was fitted to the output of the algorithm. From the normalized and detrended results we were able to find the best period.

Our third algorithm was the Gregory-Loredo Bayesian signal detection as presented in Gregory & Loredo (1992) and Gregory (1999). This method uses different step functions to calculate the likelihood for a given period based on Bayesian statistics. It is unbiased towards shape and sampling of the light curve because the step function can adopt arbitrary shapes. We used the assumption of independent Gaussian errors and directly applied the formulation given by Gregory (1999).

Each algorithm returned a best period leading to three different values after one run of the algorithms. To find the best period automatically we applied an additional program. Therein we set as an initial selection criterion that two of the three algorithms find the same period within an error range of ten per cent. Afterwards an additional run of the period search was conducted within that ten per cent range of the best period. Now a match within one per cent was required and we used a tighter spacing of the grid. With this criterion we were able to use the maxima of the periodograms independently of their power density and were able to detect variabilities with low signal-to-noise ratio. To exclude false-detection all phase-folded light curves were examined manually and non-periodics were removed.

3 RESULTS

In this section we first present the results for the member stars of IC 348 and later findings for non-members. The membership is according to Luhman et al. (2016).

If a star has a commonly used name we use this name to identify it in this section and give other identifiers as a footnote. Otherwise we use our internal numbering. The abbreviations used in this section are as following: LRL refers to Luhman et al. (1998) (and subsequent publications), HMW to Herbst et al. (2000b), CB to Cieza & Baliber (2006), and FKM to this work. When no distinct identifier is known we give the 2MASS name but continue using our identifier.



Figure 2. *BVR* image of IC 348 as observed from Jena with STK on 2014 December 8 with an integration time of 50 s in each band. The full STK field of view with a size of $52.8' \times 52.8'$ is shown. North is up and East to the left. The open cluster IC 348 is located around and within the reflection nebula south of the bright star Atik (o Per). Periodically variable members of IC 348 are marked with a (red) diamond, while all other members detected in this image are marked with a (yellow) square. Non-members for which we found a period are marked with a (white) triangle.

3.1 Periodic variables in IC 348

With the above mentioned method we were able to identify 87 photometric periodic stars in IC 348. Of those stars 33 have not been reported as periodic before. Including all previous studies (overview of Cieza & Baliber 2006) the total number of periodic variables in IC 348 is now 139 out of 478 members. The reasons for non-detections of previously known periodic variables are discussed in subsection 4.1.

Most of the stars are rotating young stars that show spot induced variability, although some periodic variabilities are due to occultations of proto-planetary discs or accretion. The results are summarized in Table A1 and the phase-folded light curves are shown in Figure A1. In the following paragraphs we will present only some notable variables.

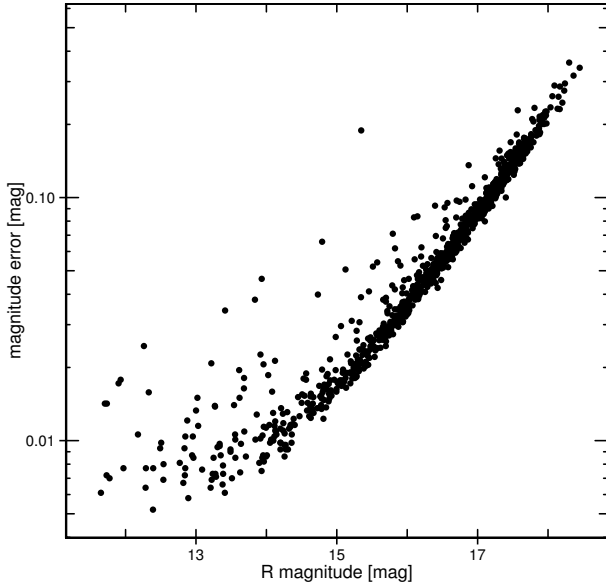


Figure 3. Photometric precision for the night of 2014 December 8 for the observations at the University Observatory Jena. This figure includes all 1001 selected stars from the FoV. In that night we also gathered *BVI* photometry of IC 348 with the STK.

3.1.1 *V695 Persei*

*V695 Per*¹ has one of the largest peak-to-peak amplitudes in our observations with 1.2 mag. The phase-folded light curve (Figure 4) resembles a typical occultation which was explained by Barsunova et al. (2013) as an AA Tauri-like system. The proto-planetary disc follows a Keplerian motion with a period of (7.55 ± 0.08) d. For the third season we observed a change in the light curve. Some data points seem to be outlier to the previously observed shape of the light curve. This is shown in the third panel of Figure 4. The outliers might be explained with a reconfiguration of the proto-planetary disc or the magnetic field. As a result the disc could be warped in a different way which leads to a change of the phase of the occultation. Alternatively an additional occultation might take place and the two effects overlap. Further monitoring of this star can help to constrain the reasons.

3.1.2 *V718 Persei*

The unusual photometric periodicity of the star *V718 Per*² was discovered by Cohen et al. (2003) and analysed in depth thereafter (Nordhagen et al. 2006b; Grinin et al. 2008). It is periodically occulted by a part of its proto-planetary disc. The occultation has a period of (4.7 ± 0.1) yr (Nordhagen et al. 2006b) while the eclipse lasts for 3.5 yr. In our data, spanning 2.4 yr, we were able to see the decrease of brightness of 0.9 mag (Figure 5). This observation shows that *V178 Per* is a rather stable system. IC 348 was monitored from Van

Table 3. Parameters of the observed transits of LRL 47. MJD_{mid} gives the midpoint of the transit as modified JD ($\text{MJD} = \text{JD} - 2456000$ d). The epoch is the orbital cycle number relative to the first observation.

Number	Depth [mag]	MJD_{mid} [d]	Epoch	Telescope
1	0.05	188.5105 ± 0.0016	0	Jena
2	0.05	203.8714 ± 0.0149	3	Tenagra
3	0.04	244.8718 ± 0.0097	11	Tenagra
4	0.07	962.2088 ± 0.0030	151	Lulin

Vleck Observatory from 1991 (Nordhagen et al. 2006b): the system was therefore observed in a stable configuration for 24 years now.

3.1.3 *A close stellar companion to LRL 47*

As well as the modulation of the flux due to starspots with a period of (4.91 ± 0.05) d, the light curve of LRL 47³ showed an additional feature. In the three observing seasons four short dips were found (see Figure 6). All of them show the typical V-shape of a grazing transit.

LRL 47 is known to be active in X-ray (Preibisch et al. 1996; Preibisch & Zinnecker 2001, 2002; Stelzer et al. 2012; Flaherty et al. 2014) like a lot of young stars are (Neuhäuser 1997). Lada et al. (2006) found no evidence of a circumstellar disc around it. Dahm (2008) and Currie & Kenyon (2009) later confirmed this result. The non-existence of a disc is not unusual for stars in IC 348. Lada et al. (2006) found a disc fraction of (50 ± 6) per cent and Cieza et al. (2007) state that discs might disappear as soon as 1 Myr after the stellar formation, building planets within this time. This star might have had a circumstellar disc which has already vanished. In addition to the non-existence of a disc, Duchêne et al. (1999) were able to exclude a stellar companion to this star with a detection limit of 3 mag at $0.5''$ (i.e. 158 AU).

The transits were observed at Jena, Tenagra, and Lulin observatories. Hence, we have three independent observations, an observational effect can therefore be excluded. These observations show again the power of the YETI network. With only a single telescope we would have missed most of the events. From the University Observatory Jena only the first event was visible and was observed. Unfortunately the *V* and *I* band observations carried out with the CTK-II mounted to the second telescope at the University Observatory Jena are not accurate enough to gain additional colour information of the transit.

The properties for the four transits are given in Table 3. The transit mid-points has been obtained with JKTEBOP (Southworth et al. 2004; Etzel 1981; Popper & Etzel 1981). Also with JKTEBOP we determined a period of (5.123874 ± 0.000063) d from those four transits. This period is close to the rotational period of (4.91 ± 0.05) d but is feasible for a close companion.

According to Luhman et al. (2003) LRL 47 is a $\text{K}0 \pm 2$ star. From the isochrones of Siess et al. (2000) we can find for the spectral type $\text{K}0$ a mass of $M_{\text{p}} = 2.7 M_{\odot}$ and a

¹ FKM 570, LRL 99, HMW 73, CB 49

² FKM 123, HMW 15, LRL 35

³ FKM 71

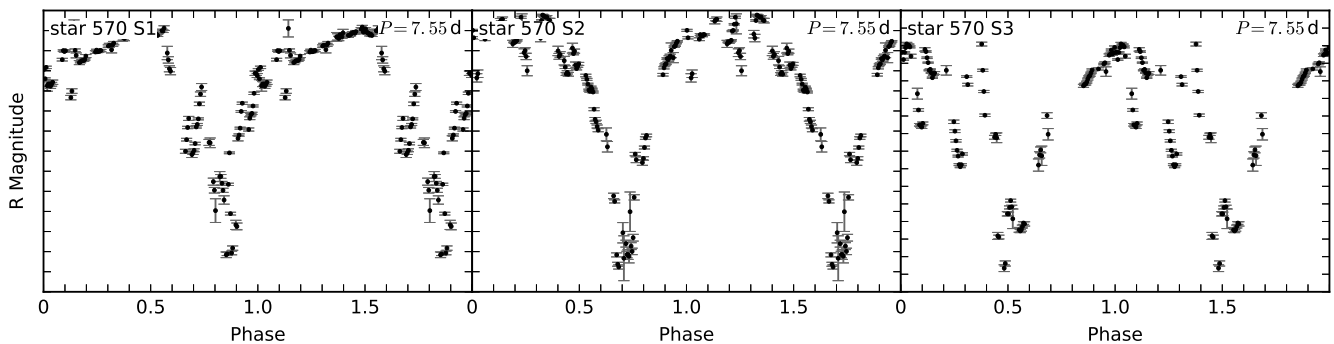


Figure 4. Phase-folded light curves of the AA Tauri-like star V695 Per for all three observing seasons. While the first two seasons are phased adequately the observations from the third season show some variability in the phase. The data has been binned and the spacing is 0.1 mag for all tick marks on the magnitude axis.

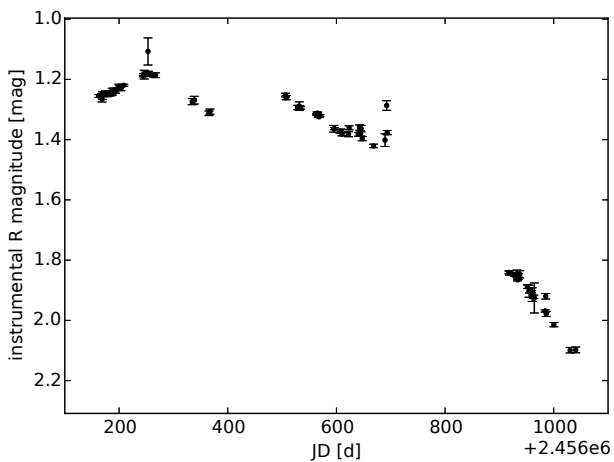


Figure 5. The full light curve of V718 Per shows the strong decrease of brightness due to the long-periodic occultation of the star. The data have been binned to one data point per night.

radius of $R_p = 4.14 R_\odot$ at the age of 2 Myr. This age is not necessarily the true age of this star. Luhman et al. (1998) gave an age-spread from 0.5 to 10 Myr for IC 348 which is under debate (see section 1). Therefore the primary’s radius can be overestimated by a factor of two. Nevertheless, we continue with the median age of 2 Myr to find an estimation of the companion’s properties.

Using JKTEBOP again for fitting the data did not lead to a satisfactory result. The reason for that is the grazing nature of the transit and our lack of additional information on the system. To get an idea of what kind the transiting object is, we assumed a Keplerian orbit and a non-grazing transit. With these assumptions we can calculate lower boundaries for the companion’s radius and mass.

First, we calculated the inclination and radius from our supposed values for the primary and the measured parameters of the transit. Thereafter we derived the mass for the companion from the low-mass isochrones of Baraffe et al. (2015). After an iterative process we concluded on an inclination of $i \lesssim 75.4^\circ$, a radius of $R_c \gtrsim 0.87 R_\odot$, and a mass of $M_c \gtrsim 0.09 M_\odot$. Here we give no uncertainties because they

would strongly underestimate the true errors. As said above those values are only lower (upper) boundaries for the mass and radius (and inclination). Due to the grazing of the transit we cannot be sure about the true radii ratio and therefore the derived values. From those lower boundaries we can conclude that this star might have a close stellar companion which might be near the hydrogen burning limit.

The four light curves show two slightly different shapes (Figure 6). The first two occurrences of the transit have a symmetric V-shape. In contrast, the later two have a steep decrease of flux at the beginning and a slower increase after the minimum. Even though two different shapes are observed we are not looking at a secondary and a primary transit. Except the first transit all have an odd orbital cycle number which rules out the double period. A secondary transit is not visible in the data of phase 0.5. This constrains the mass ratio to $\frac{M_c}{M_p} \ll 1$. The different shapes of the transit can be explained with active regions and starspots on the stellar surface.

Independent of the mass, this short period means that the companion has a small semi-major axis in the range of 0.08 AU to 0.1 AU. Therefore it is close to the primary and could not have been detected by direct imaging even using adaptive optics on a 4 m class telescope (Duchêne et al. 1999).

To constrain the mass of the companion candidate radial velocity measurements of the primary with $R = 13.5$ mag are necessary.

3.1.4 Period distribution

The distribution of the rotation periods has been an interest to all previous time-series studies of IC 348. It has always been compared to the slightly younger ONC for which Herbst et al. (2000a) discovered a bimodal period distribution. The bimodal distribution is present for more massive stars which was defined by Herbst et al. (2000a) as $M > 0.25 M_\odot$ or SpT earlier than M2 (Cohen et al. 2004) for young stars.

The comparison always gave the impression that the period distribution is similar to the period distribution of the ONC. Hence, it is bimodal with peaks for periods of about 2 d and 8 d. Despite the similarities a Kolmogorov-Smirnov test could not confirm that the two distributions (ONC and

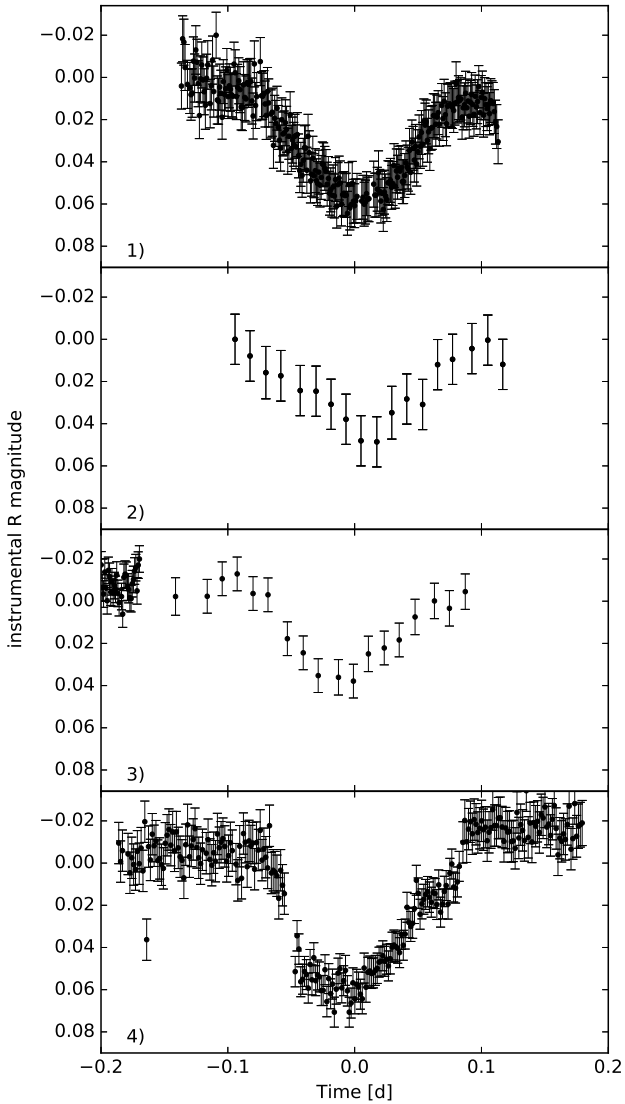


Figure 6. The light curves of the four observed transits of LRL 47 (star 71). Each is centred on the transit mid-point (see Table 3) and scaled the same for better comparison. The Tenagra telescope (2 and 3) has observed with a lower sampling than the other two telescopes (Jena/STK panel 1 and Lulin panel 4) therefore the data are sparse. In panel 3 the advantage of the YETI network is visible. The observations from two telescopes are included in this light curve. All information on the transits are listed in Table 3, including depth, duration, telescope, and time.

IC 348) are the same (Cohen et al. 2004; Littlefair et al. 2005). Furthermore, Littlefair et al. (2005) used the Hartigan dip test (Hartigan 1985; Hartigan & Hartigan 1985) and found that the bimodality in IC 348 is not statistically significant. Using the R (R Core Team 2015) implementation of the dip test (Maechler 2015) we find that the extended set of rotation periods now available has no statistically significant bimodality.

In addition to the dip test we applied two Gaussian models (Figure 7) to the data. At first we used the MASS package in R (Venables & Ripley 2002) to fit an unimodal Gaussian to the data. The second model is a mixture model

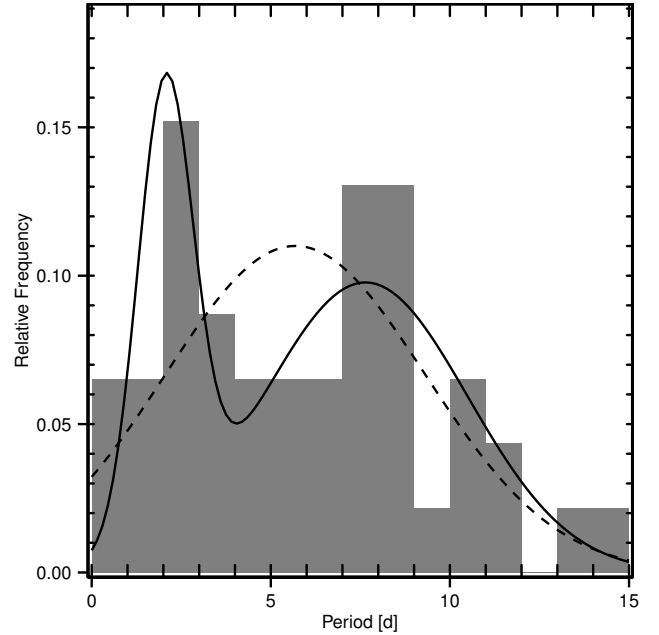


Figure 7. Period distribution of the rotation periods for high-mass stars in IC 348 (grey bars). Overlaid are a simple Gaussian model (dashed line) and a bimodal mixture model of two different Gaussians (solid line).

of two different Gaussians. To find the parameters we applied the MIXTOOLS package for R (Benaglia et al. 2009). Both models were compared to the empirical cumulative distribution function (eCDF) of the data (Figure 8). An F-test yields a p -value of $1.1 \cdot 10^{-9}$, which is the probability that the null hypothesis is true. In this case the null hypothesis is the unimodal distribution. Including all data from Cieza & Baliber (2006) the F-test yields an even smaller p -value.

We conclude that a bimodal Gaussian distribution fits more likely the data than a unimodal Gaussian distribution. Since the dip test, in contrast, favours the unimodal model the bimodality of the rotation period distribution in IC 348 is still an open issue.

Separating the rotation periods for stars with and without discs using the data from Lada et al. (2006) is also inconclusive. The low numbers of stars with discs shows a peak for the slow rotators (Figure 9) but with only two more stars than in the other bins. Among the stars without an observed disc indicator more fast rotators can be found. Nevertheless, slow rotators are among those stars, too. For the histogram in Figure 9 we used only stars which are in the group of $M > 0.25M_{\odot}$. Cieza & Baliber (2006) also found no evidence that the slow rotators preferably have discs. Even with the additional periods the statistics are still inconclusive.

For an additional regrouping we used all members with observed periods and an $H\alpha$ emission from Luhman et al. (2003). Within this sample we classified all stars with an $H\alpha$ equivalent width greater than 10 \AA as classical T-Tauri stars (cTTS) and all other as weak-lined T-Tauri stars (wTTS) (Herbig 1998)⁴. Stars without an $H\alpha$ equivalent width measurement were excluded from the sample. In Figure 10 we

⁴ Using the more detailed, spectral type-dependent classification

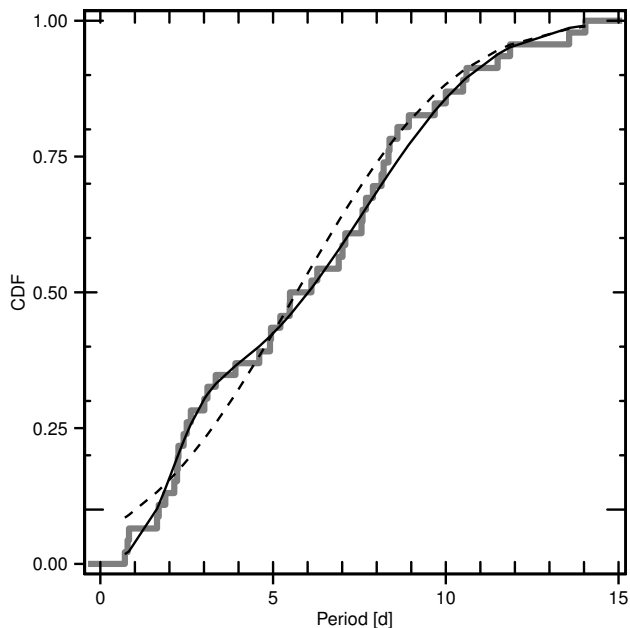


Figure 8. Cumulative distribution function (CDF) of our data. The mixture model is fitting very well. The colours and line types are the same as in Figure 7.

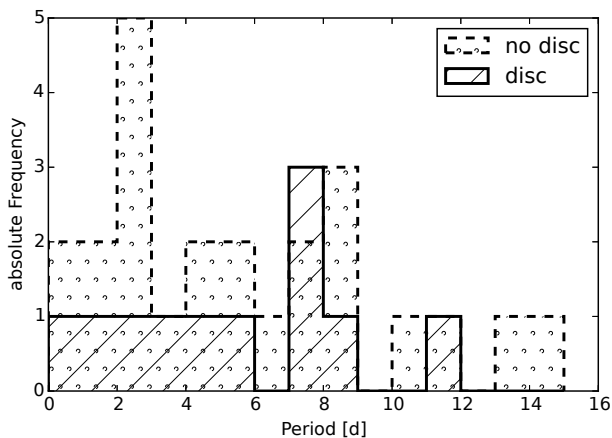


Figure 9. The period distribution of stars with $M > 0.25M_{\odot}$ separated by the existence of discs. Few discs are observed around those more massive stars in the cluster and we cannot make a statement about influence of the disc on the stellar rotation.

show the histogram of all rotation periods separated into the two groups. Due to the small amount of cTTS in our sample we have not applied statistical test to these data. From Figure 10 we can clearly see that wTTS are among slow and fast rotators. The same result was found in a much larger sample from Orion by Tanveer Karim et al. (2016), too. The

of Barrado y Navascués & Martín (2003) would not change our results and we decided to use a single critical value to distinguish between the two groups.

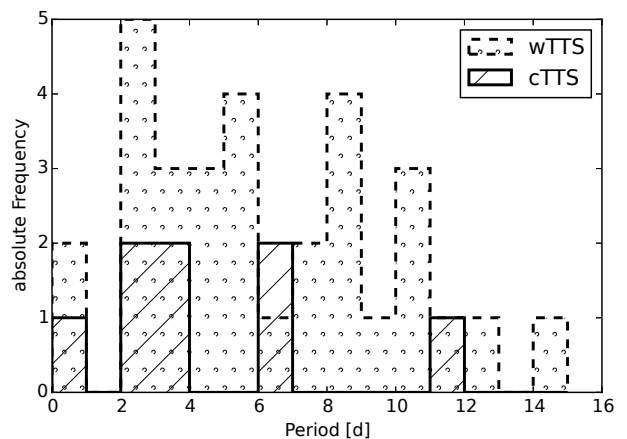


Figure 10. The period distribution of T-Tauri Stars (TTS) separated by cTTS and wTTS. Few cTTS are in our sample, but wTTS can be found in nearly all period bins.

few cTTS are distributed over the whole range of periods and we cannot find any difference between the two groups.

3.2 UX Orionis type stars in IC 348

V909 Per⁵, V712 Per⁶, and V719 Per⁷ have all been classified as UX Orionis-type stars (UXOr) by Barsunova et al. (2015). Those stars are surrounded by clumpy material in their proto-planetary disc. These clumps occults the star which leads to sudden decrease of the flux with few periodicity. From the visual inspection of the light curves we can confirm their results. For V909 Per we show the full light curve in Figure 11. In our light curves we were able to identify the same deep sudden drops as Barsunova et al. (2015). GM Cephei is a similar star which has previously been monitored by YETI (Chen et al. 2012).

While obtaining *BVRI* photometry V719 Per was covered by its disc and is therefore the faintest star in our sample $R = (18.73 \pm 0.33)$ mag. Additionally, it has a colour of $(V - R) = (2.8 \pm 0.6)$ mag and is one of the reddest stars examined. This observation seems to disagree with the properties of UXOr variables which are expected to become bluer when eclipsed. Barsunova et al. (2015) showed that V719 Per appears bluer near the photometric minimum but redder all other times during the eclipse. Our observations were obtained in the first phase of the occultation and therefore the star appeared redder.

3.3 Non-member variable stars

Within this data set we found four detached eclipsing binaries which are background stars to IC 348. They have the identifiers 213 (2MASS J03455377+3226418), 777 (CSS J034539.4+314252), 974 (CB 6), and 975 (CB 17). Only 777 is a previously known binary. The stars 975 and 974 were

⁵ FKM 78, LRL 5, HMW 20

⁶ FKM 140, LRL 37, HMW 23, CB 102

⁷ FKM 365, LRL 75, HMW 56, CB 123

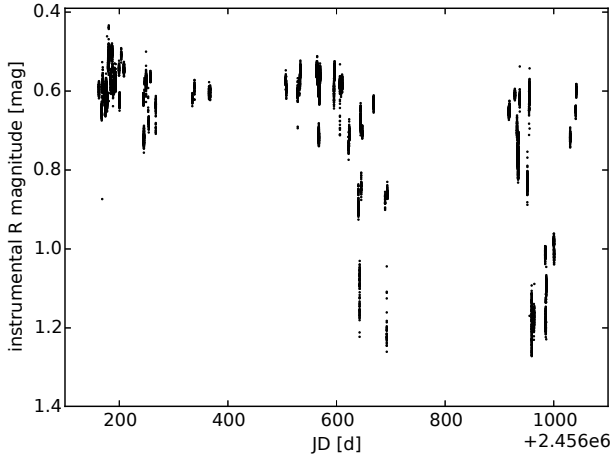


Figure 11. The UX Orionis-type star V909 Per shows sharp, sudden, non-periodic decreases of the flux. This figure includes all observations of this star.

Table 4. Periods, brightness, and colours of the four non-member eclipsing binaries found in the data. The magnitudes of the stars 974 and 975 are from [Scholz et al. \(1999\)](#).

ID	Period [d]	R [mag]	$(V - R)$ [mag]
213	0.4340 ± 0.0015	15.02 ± 0.02	0.95 ± 0.21
777	0.4882 ± 0.0015	17.26 ± 0.10	0.93 ± 0.30
974	0.422 ± 0.002	15.41 ± 0.02	0.98 ± 0.21
975	0.446 ± 0.002	15.72 ± 0.02	0.92 ± 0.21

studied by [Cieza & Baliber \(2006\)](#), though incorrect periods were stated and the binarity was not mentioned. Therefore, we can conclude that the binarity of this system was unknown before. Of those four stars all but 213 might be W UMa type binaries. The minima of 213 have rather different depths, therefore it might be a different type of detached binary.

With our data we found for 777 a period of (0.4882 ± 0.0015) d which is consistent with the value of 0.48825 d given by [Drake et al. \(2014\)](#). The periods of all four binaries are listed in [Table 4](#) and all four phase-folded light curves are presented [Figure 12](#).

Among the field stars the star 55 (NSVS J0343111+321746) is a quasi-periodic variable. [Woźniak et al. \(2004\)](#) found a period of 300 d for this star and classified it as a $SR+L$ AGB star. The period cannot be confirmed because we limited our search range to 293 d. Nevertheless, this star shows clearly a quasi-periodic variability as visible from the light curve in [Figure 13](#). The classification as a $SR+L$ AGB star can be confirmed.

3.4 Stability of periods

[Cohen et al. \(2004\)](#) reported that they found not a single variable star in IC 348 with a coherent phase for more than one observational season. In contrast [Rebull \(2001\)](#) found ~ 30 per cent of the stars in the similar aged flanking fields

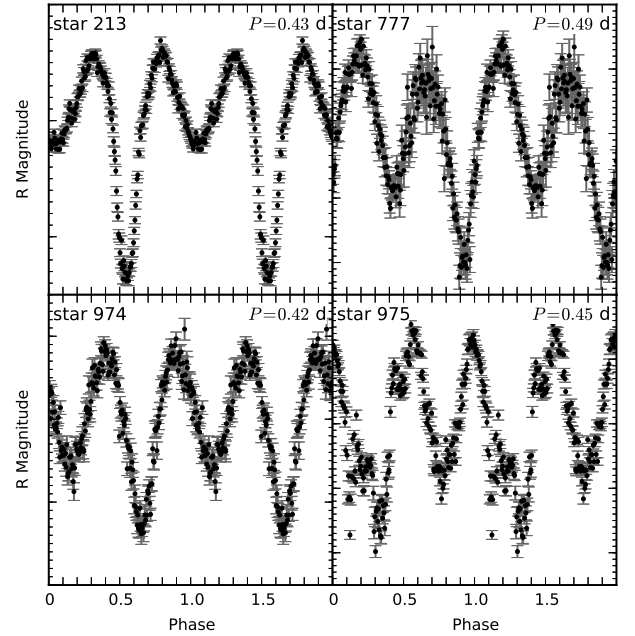


Figure 12. Phase-folded light curves of the four detached binaries in the field of view. Those stars are not members of IC 348. Further information is given in [Table 4](#). The spacing is 0.01 mag for minor ticks and 0.1 mag for major ticks.

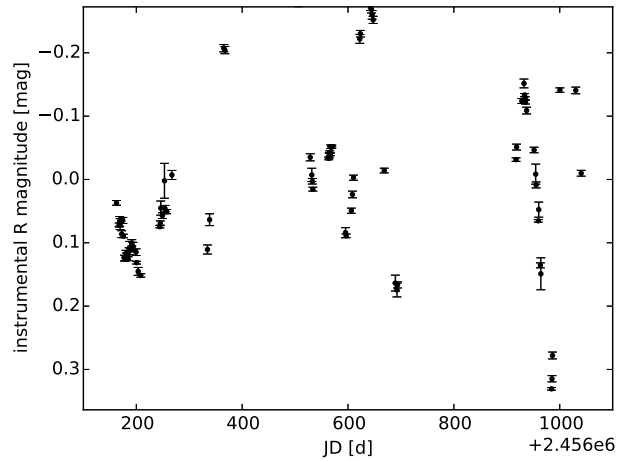


Figure 13. The full light curve of star 55 (NSVS J0343111+321746) shows quasi-periodic variability. The data have been binned to one data point per night.

of ONC to be stable up to one year. In this study we can report coherent phases of the stars in IC 348. Overall 48 per cent of the members have a coherent phase over the range of 2.4 yr.

This behaviour can be seen in [Figure A1](#) where we show the phase-folded light curves of the photometric periodic IC 348 members. All stars which have a season number added to their name have not been observed in a coherent phase over all three seasons.

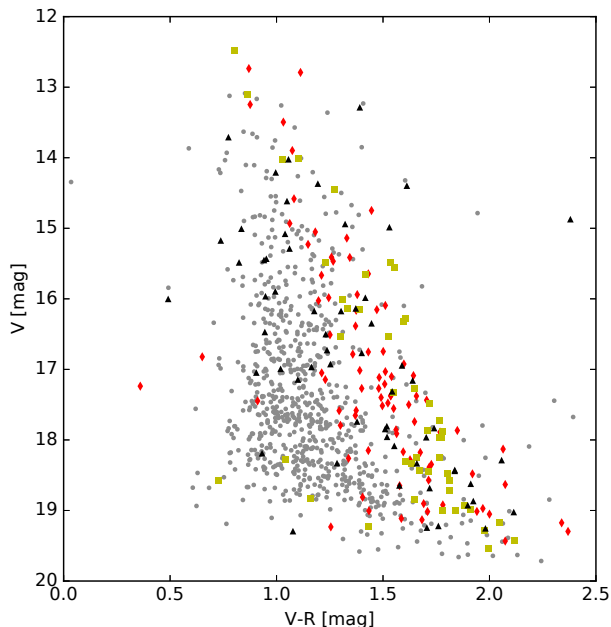


Figure 14. Colour-magnitude-diagram of our field of view. The stars are marked with the same symbols as in Figure 2 (except that the periodic non-members are marked in black instead of white) and the field stars are added with light grey circles. The cluster sequence is clearly visible. The overlap of the cluster sequence with other periodically variable stars is due to the extinction towards IC 348 (see text).

3.5 Colour-Magnitude-Diagram

In Figure 14 we present the colour-magnitude-diagram (CMD) of the whole FoV as measured from our V and R images. The diagram has not been dereddened and presents the observed colours and magnitudes. In this figure we marked the periodic stars as well as the members of IC 348. The members form a well defined cluster sequence. Some outlier are bluer than expected. Those stars are located close to the bright star Atik (α Per), which may explain the anomalous colour measurements.

In addition to the members on the cluster sequence a lot of photometric periodic stars, which are not members of the cluster, have similar positions in the CMD. Nevertheless most of those stars have sky positions which do not correspond to the position of IC 348 (Figure 2). Those stars are reddened by the medium around IC 348 and are background stars. Only two stars on the cluster sequence have a sky position corresponding with IC 348. One of them, LRL 77 (80), has been classified by Luhman et al. (2003) as a foreground star from proper motion. Our period of $P = 15.3 d$ confirms this classification. This period is too long for a typical member of the cluster. The other one star 607 ([PSZ2003] J034450.0+320345, Preibisch et al. 2003) is positioned on the southern outskirts of the cluster and we find a period of $P = 200 d$. In conclusion, none of the non-members near the sky position of the cluster and on the cluster sequence in the CMD is an unidentified member.

4 DISCUSSION

From the long-term photometry of the young open cluster IC 348 we found various periodic variable stars. For all periods given in Table A1 the systematic error is 1 per cent of the given period. This systematic error arises through the selection process of the best period. In our selection algorithm two periods are consistent if they differ by less than 1 per cent. Therefore, the true period can have an error of up to 1 per cent. For short periods the phase difference of small errors is percentually bigger than for long periods. Therefore, a short period can be determined more accurately. In contrast to this strong confinement from the periodogram rotating stars do not exhibit such a well defined periodicity. Due to the evolution of starspots a measurement error is introduced. This error is hard to estimate because it arises from physical processes in the star, with unknown properties for this particular star. Measuring the period of a differentially rotating star can lead to results differing as much as 10 per cent (s. subsection 4.1). A 1 per cent error is therefore a reasonable estimate even for fast rotating stars.

The periodicity of binary stars can be determined with greater accuracy because the orbital period is not subject to phase changes. If it is possible from the periodograms we give smaller errors for those stars in Table A1.

4.1 Comparison with previous work

In the previous work of Cieza & Baliber (2006) all known periods have been merged into a single data set. From this base we can compare our results with the known periods. The comparison with Cieza & Baliber (2006) shows that our method is reliable. Only six periods found in both works differ strongly. When phase-folding our light curves with the period given by Cieza & Baliber (2006) we cannot see any coherent behaviour in the light curve. The periods given by Cieza & Baliber (2006) might suffer from beating with the sampling rate. A very special case is the star 968 (CB 62, LRL 72) for which the authors gave a period of 1 d which is very likely an alias period, since the observations were carried out in a few nights at one observatory. Our data with a better phase coverage show a periodicity of $(44.6 \pm 0.5) d$.

For all other stars found in both studies the periods match well with the line of equality, or in some cases have a ratio of 1:2 or 2:1 (Figure 15). Some periods differ by 0.3 d which can be explained by differentially rotating stars and spot evolution (see Rebull 2001 and Cieza & Baliber 2006).

For 24 stars for which Cieza & Baliber (2006) gave a period we were not able to find any periodic variability. Given the activity of the young stars this is not a surprising result. Several reasons can lead to a non-detection. On the one hand the star might have shown no periodic behaviour over the course of three years. Some observed stars were periodic only in one out of three seasons and a lot of stars are not periodic at all, which does not mean that no starspots were present. The stars are still very variable, but no periodicity can be detected because of the number or the evolution of the starspots. For the stars which showed no periodic variability Jackson & Jeffries (2012) found in NGC 2516 no qualitative difference to stars which did. Therefore it is not unusual to miss rotational periods published before. For the same reason it was possible to find 25 new rotation periods

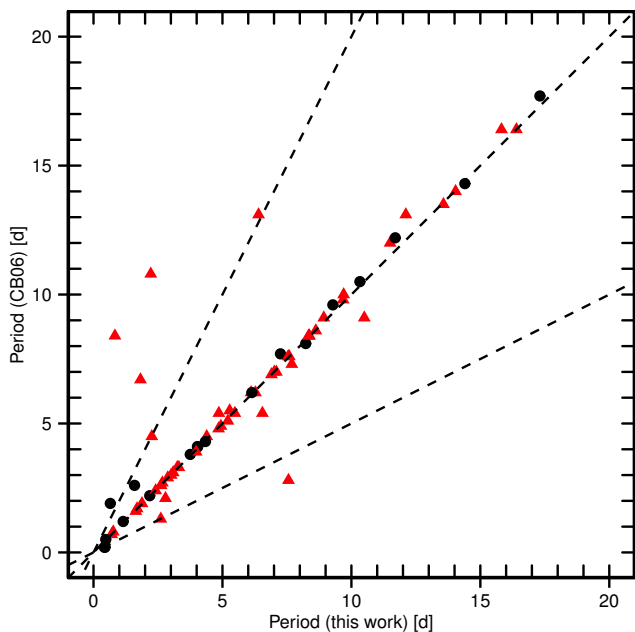


Figure 15. Comparison of our periods to the data of Cieza & Baliber (2006) (CB06). The (red) triangles represent members of IC 348 and (black) dots are field stars. The dotted lines correspond to the relations of 1:2, 1:1 and 2:1 (from top to bottom).

although IC 348 is well researched. On the other hand the variability due to spots can easily be covered by other non-periodic behaviours. If the noise in terms of erratic behaviour of the light curve is too strong, even the best algorithms cannot find the underlying period in the light curve.

Cieza & Baliber (2006) stated the number of periodic stars in IC 348 to be 143. This included 37 stars not listed as members in Luhman et al. (2003). With the membership criterion of Cieza & Baliber (2006) (everything in the FoV of their study, including foreground and background objects) the number of stars in IC 348 which have shown some periodicity is around 200.

4.2 Further periodic variables in the field of view

The case of LRL 47 shows the importance of the long-term monitoring of young open clusters for finding companions. Although, the periodicity of the observed transit is 5.12 d it was observed only four times over three observing seasons. Other surveys have missed this event before and we were only able to calculate a period because we used observations distributed through YETI at observatories worldwide.

By analysing the whole FoV and not just the members of the cluster we were able to find additional periodic stars, including three unknown contact binaries. This shows there is additional scientific value in analysing all available data, and not just primary targets (in this case the stars associated with the cluster).

5 CONCLUSIONS

With long-term photometry from different telescopes worldwide we were able to identify 148 periodic variabilities in our FoV centred at IC 348. Because of the long time-scale and the wide FoV 74 of the periods are newly discovered. This includes 33 new periodic variables in IC 348. The total number of periodic stars among the members of IC 348 (counting only the stars of Luhman et al. (2016)) rises with this study to 139. Discovering new periods in this well studied cluster is possible due to the high variability of the starspots on these young stars. With a time base large enough it should be possible to determine rotational periods for most stars in young clusters. Photometric long-term studies are therefore viable sources of statistically significant data on the rotation of stars.

With the additional periods for the stars in IC 348 we were able to show that a bimodal Gaussian distribution fits the data more likely than a unimodal. Nevertheless, a dip test was inconclusive and we have no statistical evidence that the period distribution of the stars in IC 348 is bimodal. In addition we showed that for the stars of IC 348 the rotation period does not depend on the type of the T-Tauri stars (TTS). Weak-lined and classical TTS can both be found among fast and slow rotators. The same applies to stars with and without an observed disc indicator. Stars without a disc can also be found among the slow rotators.

For LRL 47 we found a close low-mass stellar companion. The companion has been observed in a grazing transit hence our analysis from single-band photometric data is not reliable. For further characterization of this system – including mass determination – radial velocity data are desirable.

Outside the cluster we discovered three previously unknown background detached binaries and were able to confirm the period of a fourth.

ACKNOWLEDGMENTS

We would like to thank the anonymous referee for the helpful comments which improved and clarified the paper. We are grateful to D. Cohen and E. Jensen for obtaining valuable observations at the Peter van de Kamp observatory, Swarthmore College and Y. Oasa at Saitama University Observatory. We thank A. Dathe, A. Ide, D. Keeley, W. Pfau, S. Schönfeld, and L. Trepl for observing at the University Observatory Jena. Based on observations obtained with telescopes of the University Observatory Jena, which is operated by the Astrophysical Institute and University-Observatory of the Friedrich-Schiller-University, and on observations obtained at the Llano del Hato National Astronomical Observatory of Venezuela, operated by the Centro de Investigaciones de Astronomía (CIDA) for the Ministerio del Poder Popular para la Ciencia y Tecnología. We would like to thank the Thuringian State (Thüringer Ministerium für Bildung, Wissenschaft und Kultur) in project number B 515-07010 for financial support. MK thanks RN and Prof. R. Redmer in DFG projects NE 515 / 34-1 & 2 and RE 882 / 12-2, respectively, both in SPP 1385. CA thanks RN in DFG projects NE 515 / 35-1 & 2 in SPP 1385. TB and RWW are grateful to the Science and Technology Facilities Committee (STFC) for financial support (grant reference ST/J001236/1). BD thanks

RN in DFG project C2 in SFB-TR 7. RE thanks RN in DFG projects NE 515 / 34-1 & 2 in SPP 1385. CG thanks MM in DFG project MU 2695 / 18-1. CM thanks K. Schreyer in DFG project SCHR 665 / 7-1. AP thanks RN in DFG project C2 in SFB-TR 7. SR thanks RN in DFG projects NE 515 / 33-1 & 2 in SPP 1385. SR is currently a Research Fellow at ESA/ESTEC. JGS thanks RN in DFG project B9 in SFB-TR 7. TOBS thanks Prof. J. Schmitt in DFG RTG 1351 *Extrasolar Planets and their Host Stars*. This work was supported by grant VEGA 2/0143/14 of Slovak Academy of Sciences. IRAF is distributed by the National Optical Astronomy Observatories, which are operated by the Association of Universities for Research in Astronomy, Inc., under cooperative agreement with the National Science Foundation. This research has made use of NASA's Astrophysics Data System. This research has made use of the VizieR catalogue access tool and SIMBAD database, both operated at CDS, Strasbourg, France. The original description of the VizieR service was published in *A&AS* 143, 23. "The SIMBAD astronomical database" in *A&AS*, 143, 9 Wenger et al. This research has made use of TOPCAT (Taylor 2005) and astrometry.net (Lang et al. 2010). This publication makes use of data products from the Two Micron All Sky Survey, which is a joint project of the University of Massachusetts and the Infrared Processing and Analysis Center/California Institute of Technology, funded by the National Aeronautics and Space Administration and the National Science Foundation.

REFERENCES

- Attridge J. M., Herbst W., 1992, *ApJ*, **398**, L61
- Bakos G., Noyes R. W., Kovács G., Stankov K. Z., Sasselov D. D., Domsa I., 2004, *PASP*, **116**, 266
- Baraffe I., Homeier D., Allard F., Chabrier G., 2015, *A&A*, **577**, A42
- Barrado y Navascués D., Martín E. L., 2003, *AJ*, **126**, 2997
- Barsunova O. Y., Grinin V. P., Sergeev S. G., 2013, *Astrophysics*, **56**, 395
- Barsunova O. Y., Grinin V. P., Sergeev S. G., Semenov A. O., Shugarov S. Y., 2015, *Astrophysics*, **58**, 193
- Bell C. P. M., Naylor T., Mayne N. J., Jeffries R. D., Littlefair S. P., 2013, *MNRAS*, **434**, 806
- Benaglia T., Chauveau D., Hunter D. R., Young D., 2009, *Journal of Statistical Software*, **32**, 1
- Bordé P., Rouan D., Léger A., 2003, *A&A*, **405**, 1137
- Broeg C., Fernández M., Neuhäuser R., 2005, *Astronomische Nachrichten*, **326**, 134
- Chen W. P., et al., 2012, *ApJ*, **751**, 118
- Cieza L., Baliber N., 2006, *ApJ*, **649**, 862
- Cieza L., et al., 2007, *ApJ*, **667**, 308
- Cohen R. E., Herbst W., Williams E. C., 2003, *ApJ*, **596**, L243
- Cohen R. E., Herbst W., Williams E. C., 2004, *AJ*, **127**, 1602
- Currie T., Kenyon S. J., 2009, *AJ*, **138**, 703
- Dahm S. E., 2008, *AJ*, **136**, 521
- Drake A. J., et al., 2014, *ApJS*, **213**, 9
- Duchêne G., Bouvier J., Simon T., 1999, *A&A*, **343**, 831
- Dworetzky M. M., 1983, *MNRAS*, **203**, 917
- Errmann R., et al., 2014, *Astronomische Nachrichten*, **335**, 345
- Eitzel P. B., 1981, in Carling E. B., Kopal Z., eds, *Photometric and Spectroscopic Binary Systems*. p. 111
- Flaherty K. M., et al., 2014, *ApJ*, **793**, 2
- Garai Z., et al., 2016, *Astronomische Nachrichten*, **337**, 261
- Gregory P. C., 1999, *ApJ*, **520**, 361
- Gregory P. C., Loredó T. J., 1992, *ApJ*, **398**, 146
- Grinin V. P., Stempels H. C., Gahm G. F., Sergeev S., Arkharov A., Barsunova O., Tambovtseva L., 2008, *A&A*, **489**, 1233
- Hardy L. K., Butterley T., Dhillon V. S., Littlefair S. P., Wilson R. W., 2015, *MNRAS*, **454**, 4316
- Hartigan P. M., 1985, *Journal of the Royal Statistical Society. Series C (Applied Statistics)*, **34**, 320
- Hartigan J. A., Hartigan P. M., 1985, *The Annals of Statistics*, **13**, 70
- Herbig G. H., 1954, *PASP*, **66**, 19
- Herbig G. H., 1998, *ApJ*, **497**, 736
- Herbst W., Rhode K. L., Hillenbrand L. A., Curran G., 2000a, *AJ*, **119**, 261
- Herbst W., Maley J. A., Williams E. C., 2000b, *AJ*, **120**, 349
- Jackson R. J., Jeffries R. D., 2012, *MNRAS*, **423**, 2966
- Jeffries R. D., Littlefair S. P., Naylor T., Mayne N. J., 2011, *MNRAS*, **418**, 1948
- Lada C. J., et al., 2006, *AJ*, **131**, 1574
- Lang D., Hogg D. W., Mierle K., Blanton M., Roweis S., 2010, *AJ*, **139**, 1782
- Littlefair S. P., Naylor T., Burningham B., Jeffries R. D., 2005, *MNRAS*, **358**, 341
- Luhman K. L., Rieke G. H., Lada C. J., Lada E. A., 1998, *ApJ*, **508**, 347
- Luhman K. L., Stauffer J. R., Muench A. A., Rieke G. H., Lada E. A., Bouvier J., Lada C. J., 2003, *ApJ*, **593**, 1093
- Luhman K. L., Esplin T. L., Loutrel N. P., 2016, preprint ([arXiv:1605.08907](https://arxiv.org/abs/1605.08907))
- Maechler M., 2015, diptest: Hartigan's Dip Test Statistic for Unimodality - Corrected. <http://CRAN.R-project.org/package=dipstest>
- Mugrauer M., 2016, *Astronomische Nachrichten*, **337**, 226
- Mugrauer M., Berthold T., 2010, *Astronomische Nachrichten*, **331**, 449
- Neuhäuser R., 1997, *Science*, **276**, 1363
- Neuhäuser R., et al., 2011, *Astronomische Nachrichten*, **332**, 547
- Nordhagen S., Herbst W., Rhode K. L., Williams E. C., 2006a, *AJ*, **132**, 1555
- Nordhagen S., Herbst W., Williams E. C., Semkov E., 2006b, *ApJ*, **646**, L151
- Nutzman P., Charbonneau D., 2008, *PASP*, **120**, 317
- Popper D. M., Eitzel P. B., 1981, *AJ*, **86**, 102
- Preibisch T., Zinnecker H., 2001, *AJ*, **122**, 866
- Preibisch T., Zinnecker H., 2002, *AJ*, **123**, 1613
- Preibisch T., Zinnecker H., Herbig G. H., 1996, *A&A*, **310**, 456
- Preibisch T., Stanke T., Zinnecker H., 2003, *A&A*, **409**, 147
- R Core Team 2015, R: A Language and Environment for Statistical Computing. R Foundation for Statistical Computing, Vienna, Austria, <http://www.R-project.org/>
- Rebull L. M., 2001, *AJ*, **121**, 1676
- Ricker G. R., et al., 2014, in *Space Telescopes and Instrumentation 2014: Optical, Infrared, and Millimeter Wave*. p. 914320 ([arXiv:1406.0151](https://arxiv.org/abs/1406.0151)), doi:10.1117/12.2063489
- Scholz R.-D., et al., 1999, *A&AS*, **137**, 305
- Siess L., Dufour E., Forestini M., 2000, *A&A*, **358**, 593
- Southworth J., Maxted P. F. L., Smalley B., 2004, *MNRAS*, **351**, 1277
- Stelzer B., Preibisch T., Alexander F., Mucciarelli P., Flaccomio E., Micela G., Sciortino S., 2012, *A&A*, **537**, A135
- Tanveer Karim M., et al., 2016, preprint, ([arXiv:1605.04333](https://arxiv.org/abs/1605.04333))
- Taylor M. B., 2005, in Shopbell P., Britton M., Ebert R., eds, *Astronomical Society of the Pacific Conference Series Vol. 347, Astronomical Data Analysis Software and Systems XIV*. p. 29
- Trullols E., Jordi C., 1997, *A&A*, **324**, 549
- Venables W. N., Ripley B. D., 2002, *Modern Applied Statistics with S*, fourth edn. Springer, New York, <http://www.stats.ox.ac.uk/pub/MASS4>

Woźniak P. R., Williams S. J., Vestrand W. T., Gupta V., 2004, [AJ](#), **128**, 2965
Zechmeister M., Kürster M., 2009, [A&A](#), **496**, 577

APPENDIX A: COMPLETE LIST OF RESULTS

In the appendix we present a table of our results for all periodically variable stars in the FoV and the phase-folded light curves for all periodically variable stars among the IC 348 members.

This paper has been typeset from a $\text{\TeX}/\text{\LaTeX}$ file prepared by the author.

Table A1. Here we present all periods (members and non-members) found in our data. *ID* gives the number used in this paper, *Identifier* is a name from 2MASS or [Preibisch et al. \(2003\)](#). *CB* and *LRL* are the IDs of [Cieza & Baliber \(2006\)](#) and [Luhman et al. \(1998\)](#), respectively. Stars with an LRL ID in parenthesis are non-members of IC 348 according to [Luhman et al. \(2003\)](#), other stars with an LRL ID are members from [Luhman et al. \(2016\)](#). *P* states our period with the error ΔP while P_{CB} is the value given by [Cieza & Baliber \(2006\)](#). *Amplitude* gives the peak-to-peak amplitude of the periodic light curve in magnitudes. *R* and $(V - R)$ are in the Bessel system and have been measured from our data.

ID	RA [°]	DEC [°]	Identifier	CB	LRL	<i>P</i> [d]	ΔP [d]	P_{CB} [d]	Amplitude [mag]	<i>R</i> [mag]	$(V - R)$ [mag]
25	56.1632	32.1552	2MASS J03443916+3209182	109	9	1.64	0.02	1.6	0.094	13.3	1.4
27	56.1539	32.1127	2MASS J03443694+3206453	95	6	1.69	0.02	1.7	0.072	11.7	1.1
30	55.9635	32.2193	2MASS J03435123+3213091		22	0.788	0.003		0.12	11.9	0.9
31	55.8851	32.5134	2MASS J03433241+3230477			0.78	0.01		0.019	11.9	1.4
36	56.1000	32.1834	2MASS J03442398+3211000		38	0.71	0.01		0.027	12.4	0.9
38	55.7496	32.1541	2MASS J03425992+3209144			45.5	0.5		0.21	12.5	2.4
49	55.5409	32.3859	2MASS J03420982+3223086			39.1	0.4		0.16	12.8	1.6
52	55.5155	32.2742	2MASS J03420373+3216269			0.1132	0.001		0.012	12.9	0.8
54	55.4924	32.2384	2MASS J03415816+3214179			4.13	0.04		0.10	13.0	1.1
60	55.8956	32.5271	2MASS J03433494+3231372			0.84	0.01		0.055	13.2	1.2
67	56.0684	32.1654	2MASS J03441642+3209552	45	53	3.01	0.03	3	0.15	13.2	1.0
71	55.9813	32.1590	2MASS J03435550+3209321		47	4.91	0.05		0.88	13.5	1.1
72	55.7439	32.4100	2MASS J03425852+3224359			32.7	0.3		0.15	13.5	1.5
80	56.1809	32.1382	2MASS J03444342+3208172		(77)	15.3	0.2		0.077	13.6	1.0
84	55.4940	32.0440	2MASS J03415855+3202379			11.51	0.12		0.088	13.6	1.3
87	56.1462	32.1270	2MASS J03443503+3207370	91	24 A	2.26	0.02	4.5	0.12	13.8	1.3
95	56.0209	32.1650	2MASS J03440499+3209537		56	21.5	0.2		0.063	13.9	1.2
98	56.2563	32.1810	2MASS J03450151+3210512	133	79	1.88	0.02	1.9	0.071	13.9	1.1
107	56.1452	32.1093	2MASS J03443487+3206337	89	48	5.48	0.05	5.4	0.15	14.2	1.3
109	55.7419	32.3678	2MASS J03425806+3222042			28.1	0.3		0.028	14.0	1.0
110	56.0369	32.2697	2MASS J03440885+3216105		44	7.89	0.08		0.053	14.1	1.3
112	56.3775	32.0322	2MASS J03453061+3201557		10363	2.24	0.02		0.084	14.1	1.1
118	56.1186	32.1230	2MASS J03442847+3207224	76	66	7.01	0.07	7	0.17	14.2	1.3
125	56.1602	32.1266	2MASS J03443845+3207356	104	36	5.21	0.05	5.1	0.27	14.2	1.4
126	55.5462	32.3783	2MASS J03421109+3222418			11.0	0.1		0.05	14.2	1.1
139	56.4865	32.1620	2MASS J03455676+3209428			1.26	0.01		0.031	14.4	0.7
145	55.8836	32.1049	2MASS J03433205+3206172		94	5.49	0.05		0.18	14.5	1.2
147	56.1672	32.1928	2MASS J03444011+3211341		59	2.14	0.02		0.10	14.6	1.4
151	56.0007	32.3708	2MASS J03440015+3222144			12.15	0.12		0.028	14.5	0.9
154	56.2572	32.2411	2MASS J03450174+3214276	134	39	16.4	0.2	16.4	0.10	14.6	1.5
157	56.1066	32.2084	2MASS J03442557+3212299	68	64	8.37	0.08	8.4	0.47	14.8	1.4
158	56.4391	32.1445	2MASS J03454539+3208401			11.91	0.12		0.052	14.7	0.8
162	55.7459	32.5015	2MASS J03425901+3230053			21.0	0.2		0.054	14.6	1.4
163	56.1126	32.0789	2MASS J03442702+3204436	71	69	8.93	0.09	9.1	0.20	14.7	1.2
168	55.6818	31.9876	2MASS J03424360+3159150	10		2.18	0.02	2.2	0.094	14.8	1.4
174	56.1775	32.1055	2MASS J03444261+3206194	121	146	11.5	0.1	12	0.16	14.8	1.2
176	56.1558	32.1033	2MASS J03443740+3206118	97	82	6.28	0.06	6.2	0.095	15.0	1.4
184	56.3166	32.5146	2MASS J03451598+3230519	135		4.04	0.04	4.1	0.12	14.9	1.4
187	55.9618	31.9059	2MASS J03435084+3154210			4.04	0.04		0.12	14.9	1.3
190	56.4079	32.1403	2MASS J03453789+3208249			0.28	0.01		0.012	14.9	1.0
195	55.6255	31.7028	2MASS J03423010+3142104			29.9	0.3		0.088	15.0	1.2
213	56.4741	32.4451	2MASS J03455377+3226418			0.434	0.002		0.075	15.0	0.9
217	55.6693	32.2859	2MASS J03424056+3217101			3.34	0.03		0.085	15.3	1.2
223	55.9531	32.1260	2MASS J03434875+3207332	25	111	39.1	0.4	20.3	0.07	15.3	1.3
226	56.0091	32.3278	2MASS J03440216+3219399	35	118	6.11	0.06	6.2	0.35	15.2	1.5
245	56.3181	32.1056	2MASS J03451634+3206199		1933	28.5	0.3		1.9	15.8	1.5
246	56.3474	32.4104	2MASS J03452338+3224369			8.69	0.09		0.097	15.4	1.4
251	56.0746	32.2057	2MASS J03441791+3212203	46	93	4.39	0.04	4.5	0.16	15.3	1.4
252	55.9989	32.2342	2MASS J03435970+3214028	34	87	14.04	0.1	14	0.16	15.3	1.6
260	55.9643	32.5303	2MASS J03435141+3231486	28		3.75	0.04	3.8	0.13	15.4	1.6
262	56.0476	32.3279	2MASS J03441143+3219401	41	137	0.766	0.008	0.8	0.092	15.6	1.4
268	56.0469	32.1034	2MASS J03441125+3206121	40	105	10.5	0.1	9.1	0.22	15.5	1.5
277	55.9843	32.5050	2MASS J03435622+3230178	30		8.23	0.08	8.1	0.10	15.5	1.6
279	55.6486	32.2889	2MASS J03423566+3217198	7		1.15	0.02	1.2	0.035	15.5	0.9
280	56.1172	32.2667	2MASS J03442812+3216002	75	85	2.67	0.03	2.7	0.22	15.9	1.2
282	56.1162	32.1255	2MASS J03442787+3207316	74	86	6.55	0.07	5.4	0.084	15.6	1.5
292	55.7311	31.9535	2MASS J03425546+3157123	11		0.6508	0.001	1.9	0.12	15.5	1.2

Table A1 – *continued*

ID	RA [°]	DEC [°]	Identifier	CB	LRL	P [d]	ΔP [d]	P_{CB} [d]	Amplitude [mag]	R [mag]	$(V - R)$ [mag]
296	56.1229	32.4403	2MASS J03442949+3226250			9.5	0.1		0.044	15.7	1.3
297	56.1605	32.1336	2MASS J03443854+3208006	105	58	7.69	0.08	7.3	0.20	15.7	1.7
304	56.0986	32.1130	2MASS J03442366+3206465	64	92	9.7	0.1	10	0.28	15.6	1.5
305	56.1605	32.2167	2MASS J03443838+3212597	103	144	13.5	0.1	13.5	0.27	15.8	1.5
317	55.9842	32.1434	2MASS J03435619+3208362		142	3.91	0.04		0.066	15.9	1.4
318	55.9495	32.2992	2MASS J03434788+3217567	24	126	9.68	0.1	9.8	0.16	15.7	1.5
327	56.3845	32.0542	2MASS J03453230+3203150	140	10289	0.705	0.001	0.7	0.17	15.8	1.2
341	56.0901	32.1772	2MASS J03442161+3210376	58	41	7.56	0.08	2.8	1.3	16.6	2.1
346	56.0957	32.1993	2MASS J03442297+3211572		120	5.06	0.05		0.16	15.9	1.5
347	56.1188	31.9984	2MASS J03442851+3159539		68	26.9	0.3		0.22	15.8	1.5
348	56.1384	32.2581	2MASS J03443321+3215290		122	6.96	0.07		0.098	15.7	1.7
349	56.0930	32.2002	2MASS J03442232+3212007	61	100	0.83	0.01	8.4	0.099	16.1	1.6
353	55.6923	32.4549	2MASS J03424614+3227172			12.1	0.1		0.075	16.0	1.0
355	56.1111	32.0662	2MASS J03442663+3203583	69	62	3.09	0.03	3.1	0.16	16.0	1.8
357	56.2907	32.2268	2MASS J03450986+3213350			2.47	0.02		0.03	16.0	1.1
364	56.0170	32.1214	2MASS J03440410+3207170		174	10.0	0.1		0.20	16.3	1.6
366	56.5065	32.1606	2MASS J03460161+3209375			1.67	0.02		0.087	16.1	0.9
384	56.1064	32.1920	2MASS J03442555+3211307	67	60 B	4.86	0.05	5.4	0.36	16.3	1.6
386	55.7794	32.1718	2MASS J03430704+3210182	14		6.14	0.06	6.2	0.19	16.1	1.7
387	56.1859	32.1369	2MASS J03444458+3208125		103	25.7	0.3		0.89	17.0	2.0
391	56.0898	32.1716	2MASS J03442155+3210174	56	116	7.09	0.07	7	0.36	16.1	1.8
394	55.9558	32.1778	2MASS J03434939+3210398	27	147	6.4	0.06	13.1	0.19	16.2	1.4
407	56.2123	32.2693	2MASS J03445096+3216093	128	101	12.1	0.1	13.1	0.27	16.0	1.5
421	56.0929	32.0953	2MASS J03442228+3205427	60	61	11.9	0.1	30	0.50	16.5	1.3
441	55.7352	31.7106	2MASS J03425646+3142382			8.62	0.09		0.23	16.2	2.1
444	55.5361	32.4745	2MASS J03420867+3228276			2.84	0.03		0.14	16.3	1.7
465	56.0897	32.2528	2MASS J03442156+3215098		185	8.17	0.08		0.31	16.9	0.4
470	56.2338	32.0991	2MASS J03445611+3205564	131	188	3.31	0.03	3.3	0.087	16.3	1.3
476	56.3981	31.9406	2MASS J03453551+3156257	141		9.28	0.09	9.6	0.13	16.4	1.5
477	56.1691	32.3865	2MASS J03444061+3223110	114		4.03	0.04	4.1	0.14	16.3	1.5
502	56.1023	32.0659	2MASS J03442457+3203571	65	123	4.94	0.05	4.9	0.33	17.1	1.9
505	56.2034	32.2228	2MASS J03444881+3213218	127	178	6.9	0.07	6.9	0.25	16.5	1.7
509	56.1812	32.1286	2MASS J03444351+3207427		52	8.14	0.08		0.13	16.6	1.9
514	56.2198	32.0158	2MASS J03445274+3200565		1939	10.9	0.1		0.15	16.7	1.6
523	55.9983	32.2654	2MASS J03435953+3215551	33	155	7.59	0.08	7.6	0.33	16.7	1.4
525	56.3444	31.7239	2MASS J03452267+3143259			17.1	0.2		0.15	16.4	1.4
526	55.6077	32.3507	2MASS J03422585+3221022	2		17.3	0.2	17.7	0.22	16.5	1.6
543	55.6177	32.5133	2MASS J03422824+3230479	3		4.34	0.04	4.3	0.45	16.3	1.5
544	55.9534	32.2644	2MASS J03434881+3215515	26	162	2.88	0.03	2.9	0.18	16.9	1.7
565	55.5846	32.0920	2MASS J03422033+3205310	1		7.25	0.07	7.7	0.57	16.6	1.8
570	56.0802	32.1263	PSZ2003 J034419.2+320734	49	99 A	7.55	0.08	7.6	1.3	16.0	1.5
596	56.3977	32.0572	2MASS J03453545+3203259		10284	1.57	0.02		0.26	16.6	1.6
607	56.2081	32.0628	2MASS J03444998+3203455			220	2		0.085	16.7	1.7
608	56.0906	32.2087	2MASS J03442176+3212312		180	3.26	0.03		0.08	16.7	1.7
611	56.1249	32.3230	2MASS J03442997+3219227		104	8.67	0.09		0.25	16.8	2.3
616	55.6342	31.7272	2MASS J03423219+3143382			12.2	0.1		0.21	16.7	1.9
617	55.6703	32.2264	2MASS J03424086+3213347	9		0.47375	0.00025	0.5	0.085	16.6	1.8
640	56.1495	32.2645	2MASS J03443588+3215533		181	7.7	0.08		0.17	16.6	1.7
670	56.3423	32.0345	2MASS J03452214+3202040		10373	0.78	0.01		0.10	16.9	1.3
683	56.0756	32.0825	2MASS J03441816+3204570		31	3.34	0.03		0.14	17.4	2.1
696	55.6000	31.9005	2MASS J03422398+3154016			0.579	0.001		0.07	17.0	1.3
699	56.2718	32.1653	2MASS J03450521+3209544		177	4.95	0.05		0.16	17.1	1.6
701	56.3406	32.5352	2MASS J03452174+3232065			5.07	0.05		0.2	16.9	1.9
723	56.0283	32.1318	2MASS J03440678+3207540	37	156	2.61	0.03	1.3	0.13	17.1	2.0
735	55.8874	32.4675	2MASS J03433299+3228027	22		11.7	0.1	12.2	0.23	17.3	2.0
758	56.2620	32.1169	2MASS J03450285+3207006		150	2.39	0.02		0.14	17.3	1.7
774	56.3116	32.4332	2MASS J03451480+3225594			5.58	0.06		0.2	17.0	1.9
775	56.1584	32.1937	2MASS J03443800+3211370		193	2.39	0.02		0.25	17.4	1.4
777	56.4146	31.7148	2MASS J03453948+3142528			0.4882	0.0015		0.27	17.3	0.9
796	56.1134	32.2393	2MASS J03442724+3214209		132	4.4	0.04		1.2	17.2	1.7
798	56.4449	32.4804	2MASS J03454675+3228487	143		10.33	0.1	10.5	0.20	17	1.7
800	56.1874	32.2268	2MASS J03444495+3213364		112	20.0	0.2		0.20	17.1	1.8

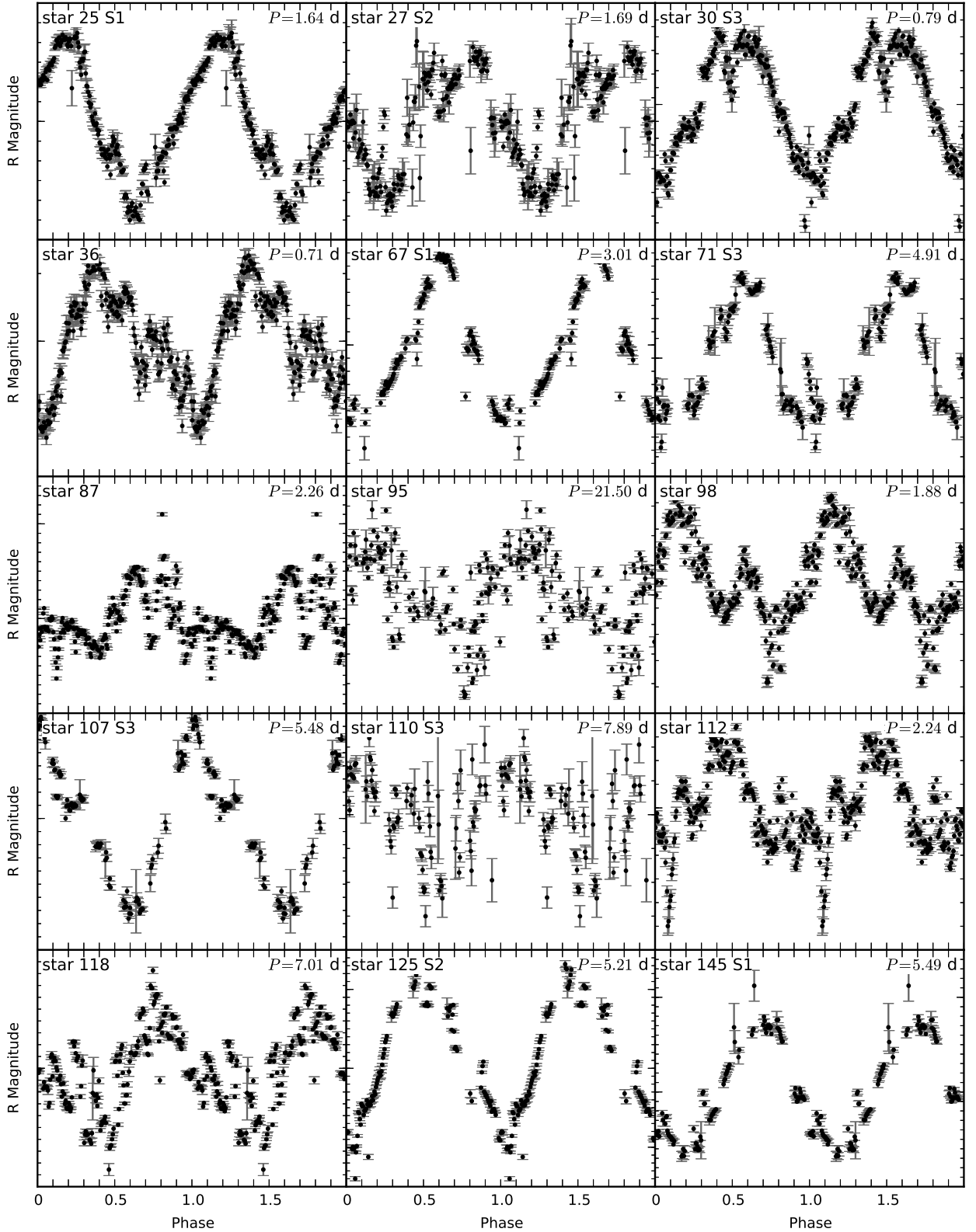


Figure A1. Phase-folded and binned (200 bins) light curves of all periodically variable IC 348 members. We present the double phase for easier visualization (data points in the phase between 1 and 2 are repeated from phase 0 to 1). For stars without a coherent phase over the full time span of the observations only one season is shown. This is indicated by S_n added to the star number, where n is an integer from 1 to 3 (compare Table 2). The spacing is 0.01 mag for minor ticks and 0.1 mag for major ticks on the magnitude axis.

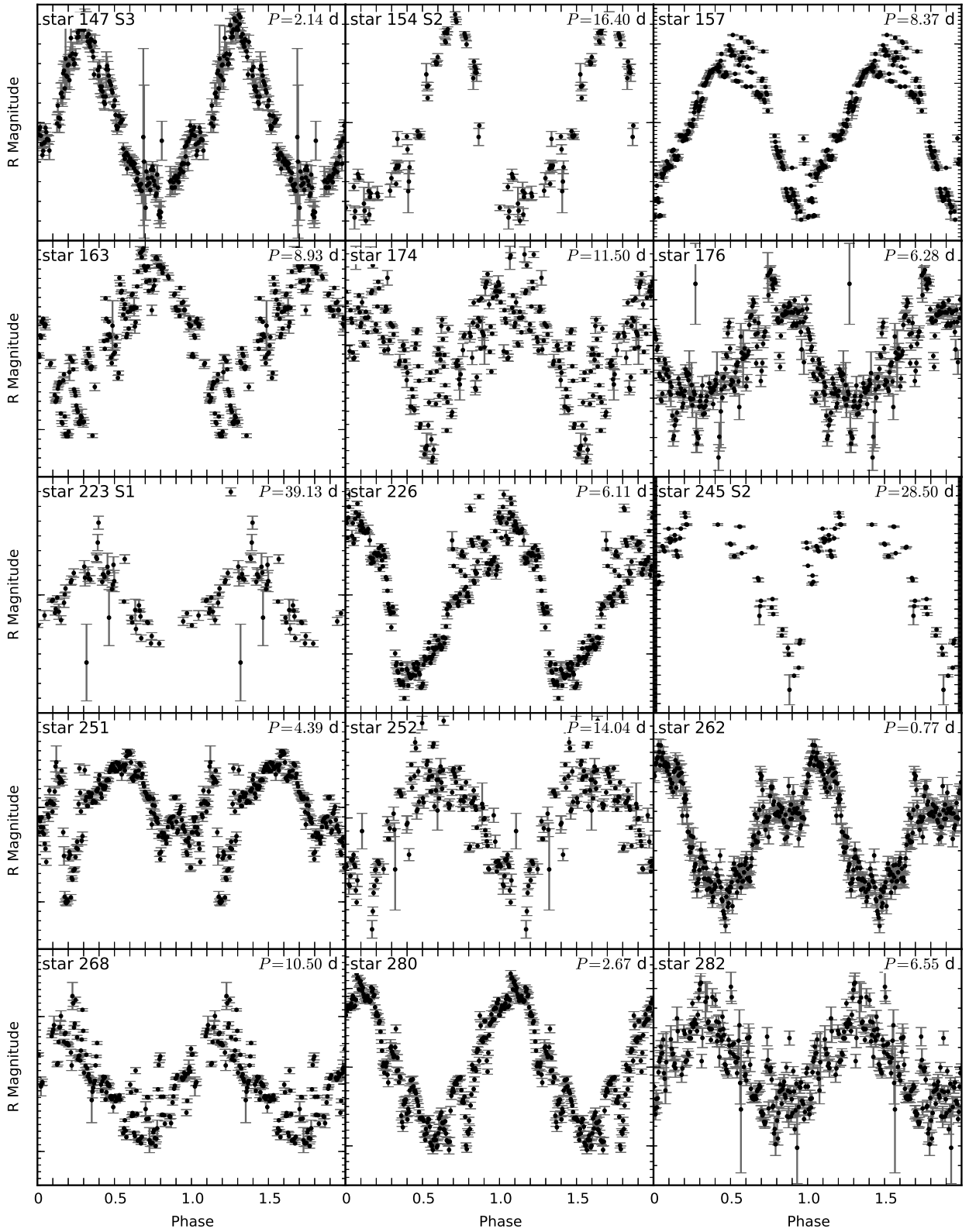


Figure A1 – continued

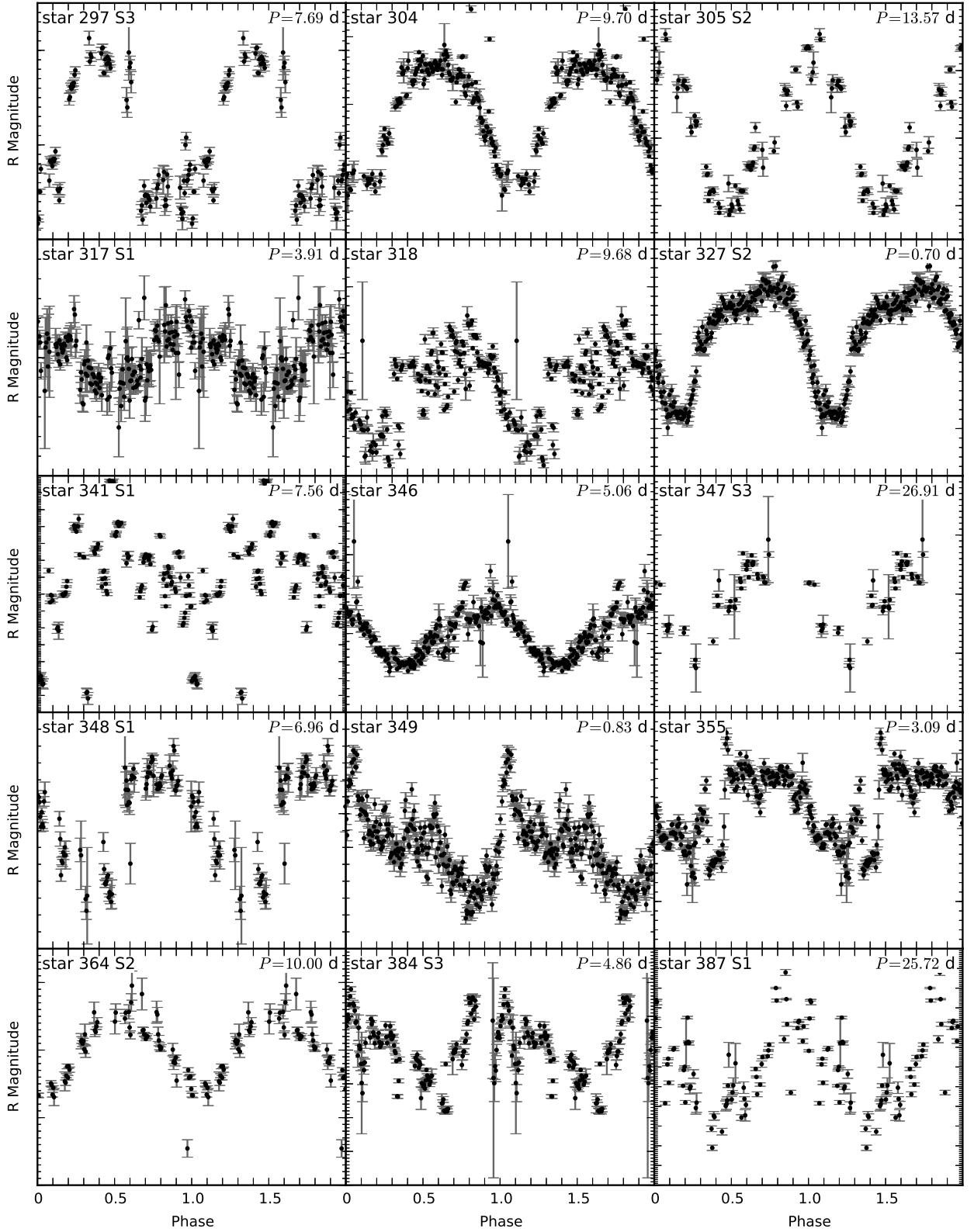


Figure A1 – continued

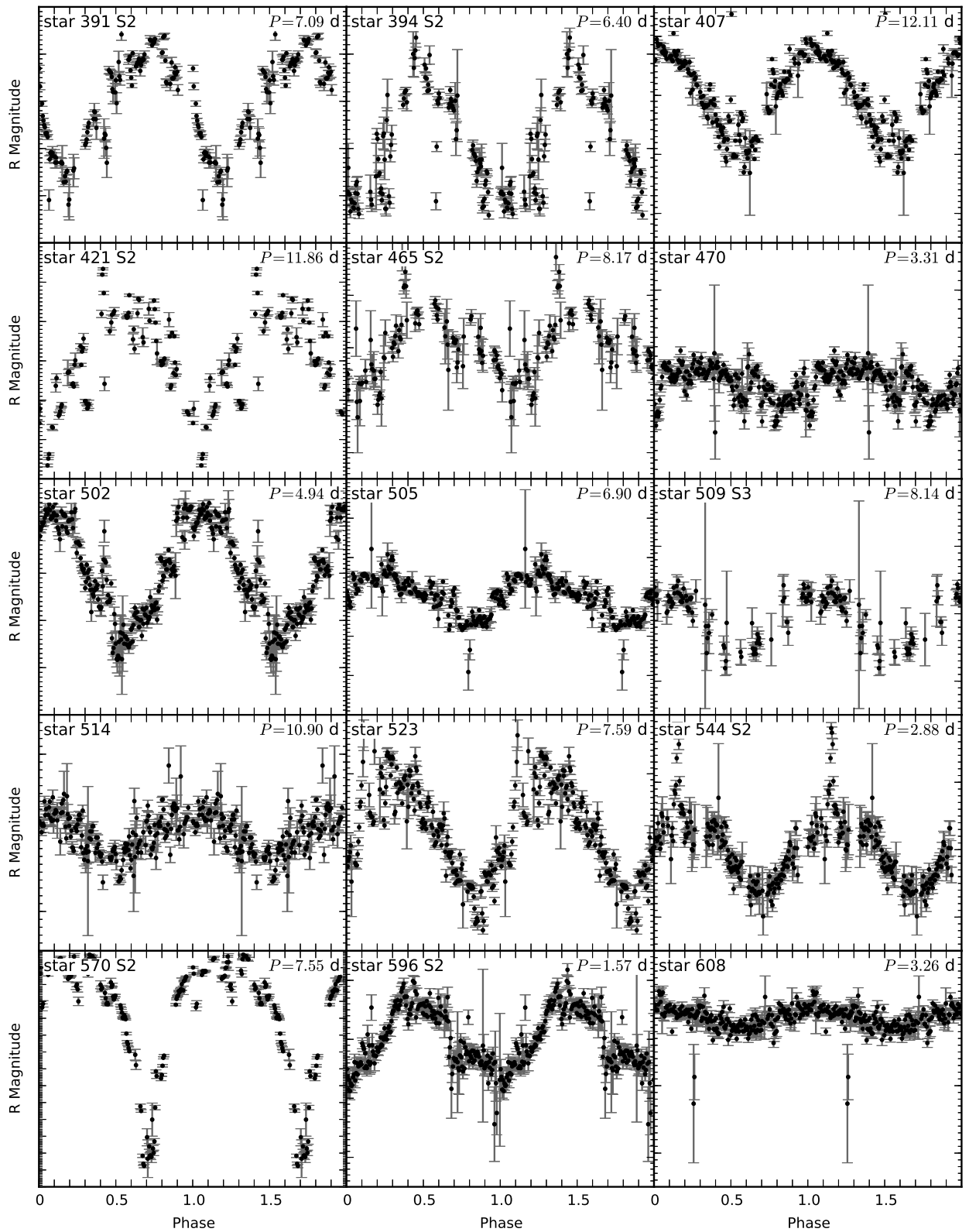


Figure A1 - continued

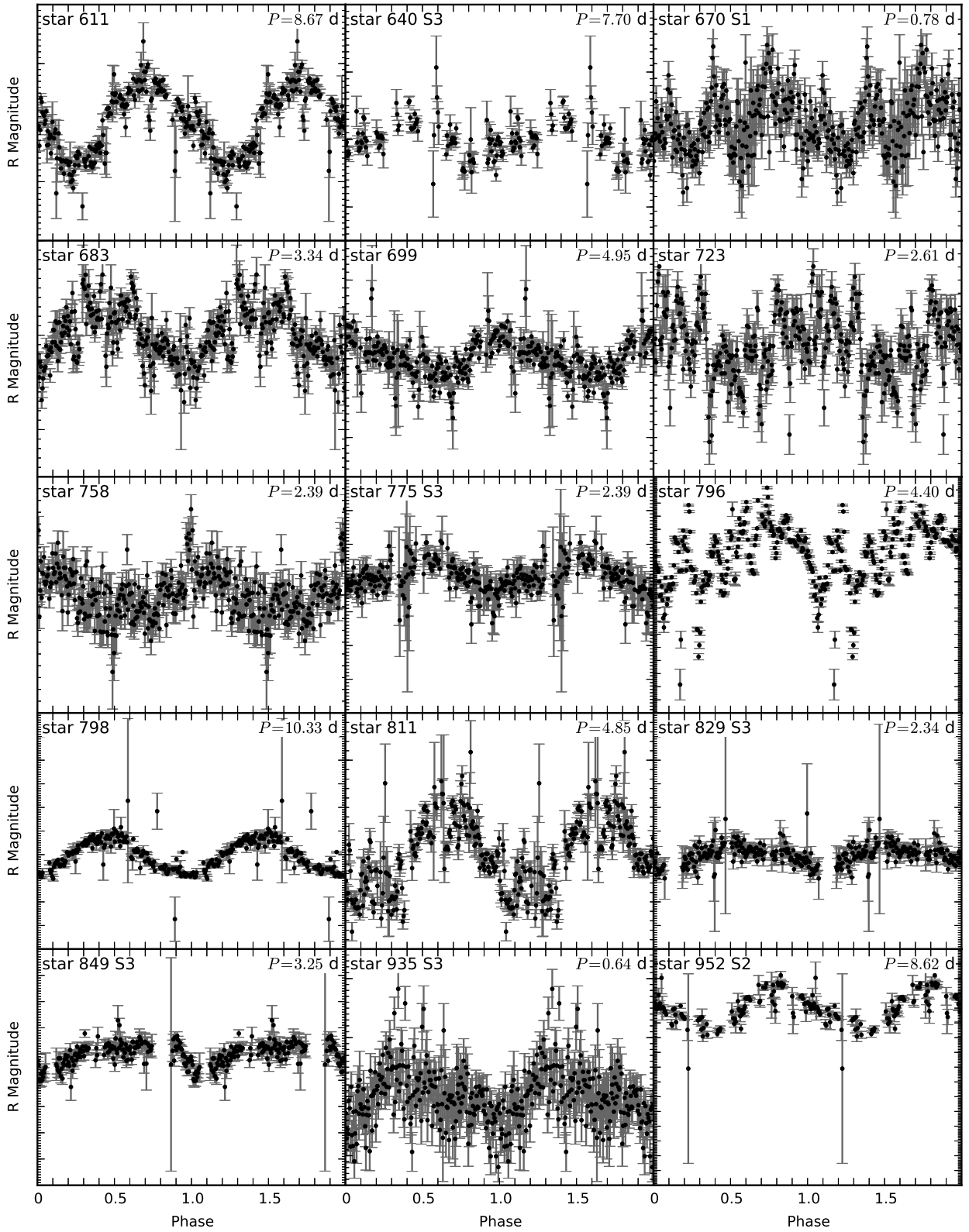


Figure A1 – continued

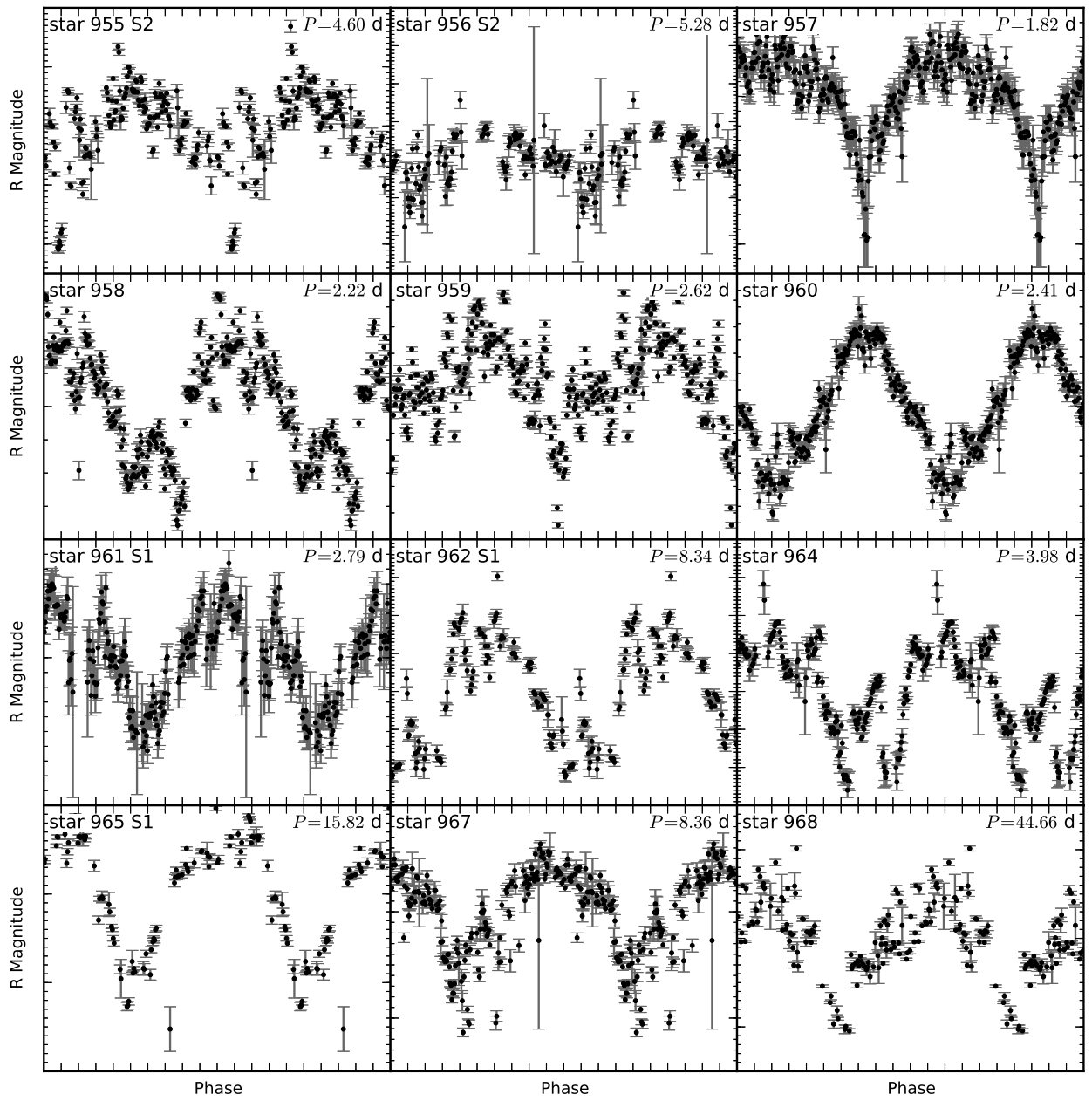
Figure A1 - *continued*

Table A1 – continued

ID	RA [°]	DEC [°]	Identifier	CB	LRL	P [d]	ΔP [d]	P_{CB} [d]	Amplitude [mag]	R [mag]	($V - R$) [mag]
807	55.6372	31.7057	2MASS J03423291+3142205			10.69	0.11		1.0	16.9	2.1
811	56.1616	32.3183	2MASS J03443878+3219056	108	208	4.85	0.05	4.8	0.20	16.9	2.4
829	56.0312	32.0691	2MASS J03440750+3204088		214	2.34	0.02		0.24	17.5	1.6
848	55.7330	31.7464	2MASS J03425593+3144463			2.46	0.02		0.12	17.1	1.6
849	56.1574	32.2050	2MASS J03443777+3212181	100	154	3.25	0.03	3.3	0.25	17.4	1.7
898	56.4328	32.4098	2MASS J03454385+3224350	142		14.4	0.1	14.3	0.30	17.5	1.8
927	56.4929	32.4466	2MASS J03455824+3226475			7.72	0.07		0.80	18.2	1.1
935	55.9526	32.2307	2MASS J03434862+3213507		261	0.638	0.006		0.30	18.0	1.3
941	56.0191	32.4684	2MASS J03440459+3228062			6.96	0.07		0.40	17.5	1.7
952	56.0834	32.1127	2MASS J03442001+3206455	50	210	8.62	0.09	8.6	0.45	17.6	1.4
955	56.1240	32.1777	2MASS J03442972+3210398		40	4.6	0.05		0.25	15.4	1.4
956	56.1363	32.1545	2MASS J03443276+3209157	82	88	5.28	0.05	5.5	0.33	16.2	0.7
957	56.1355	32.1490	2MASS J03443257+3208558	80	71	1.82	0.02	6.7	0.14	16.1	2.1
958	56.1311	32.1457	2MASS J03443153+3208449	78	29	2.22	0.02	10.8	0.069	12.8	1.1
959	56.1363	32.1438	2MASS J03443274+3208374	81	16	2.62	0.03	2.6	0.088	12.5	1.0
960	56.1611	32.1450	2MASS J03443871+3208420	107	23	2.41	0.02	2.4	0.12	15.4	1.6
961	56.1614	32.1489	2MASS J03443869+3208567	106	108	2.79	0.03	2.1	0.13	16.0	1.6
962	56.1558	32.1504	2MASS J03443741+3209009	99	83	8.34	0.08	8.4	0.43	16.5	0.9
964	56.1633	32.1623	2MASS J03443919+3209448	110	91	3.98	0.04	3.9	0.54	16.3	1.4
965	56.1416	32.1482	2MASS J03443398+3208541	86	65	15.8	0.2	16.4	0.21	14.7	1.5
967	56.0903	32.1070	2MASS J03442166+3206248	57	125	8.36	0.08	8.4	0.18		
968	56.0939	32.0314	2MASS J03442257+3201536	62	72	44.7	0.4	1	0.21	15.9	1.6
972	56.1083	32.2750	2MASS J03442595+3216306		(972)	7.56	0.08		0.032	14.2	0.8
973	56.0406	32.2868	2MASS J03440973+3217130			9.58	0.1		0.2	15.5	0.5
974	55.6466	32.5650	2MASS J03423520+3233544	6		0.422	0.002	0.2	0.25		
975	55.8014	32.5698	2MASS J03431233+3234114	17		0.446	0.002	0.20	0.35		
996	56.1153	32.5637	2MASS J03442766+3233495	73		1.59	0.02	2.6	0.094	15.8	1.5
998	56.0927	32.5625	2MASS J03442225+3233449			12.13	0.12		0.043	14.5	1.0
1001	56.4838	32.572	2MASS J03455608+3234190			11.88	0.12		0.13	15.8	1.2